Stable Isotope Trajectory Analysis (SITA): A new approach to quantify and visualize dynamics in stable isotope studies

A. Sturbois, Julien Cucherousset, M. de Cáceres, N. Desroy, P. Riera, A. Carpentier, N. Quillien, J. Grall, B. Espinasse, Y. Cherel, et al.

Received: 4 June 2021 | Revised: 21 September 2021 | Accepted: 29 September 2021

DOI: 10.1002/ecm.1501

ARTICLE

ECOLOGICAL MONOGRAPHS
ECOLOGICAL SOCIETY OF AMERICA

Stable Isotope Trajectory Analysis (SITA): A new approach to quantify and visualize dynamics in stable isotope studies

Anthony Sturbois[1,2,3,4] | **Julien Cucherousset**[5] | **Miquel De Cáceres**[6] | **Nicolas Desroy**[3] | **Pascal Riera**[7] | **Alexandre Carpentier**[8] | **Nolwenn Quillien**[9] | **Jacques Grall**[4] | **Boris Espinasse**[10] | **Yves Cherel**[11] | **Gauthier Schaal**[4]

[1]Vivarmor Nature, Ploufragan, France

[2]Réserve naturelle nationale de la Baie de Saint-Brieuc, site de l'étoile, Hillion, France

[3]Ifremer, Laboratoire Environnement et Ressources Bretagne nord, Dinard, France

[4]Laboratoire des Sciences de l'Environnement Marin (LEMAR), UMR 6539 CNRS/UBO/IRD/IFREMER, Plouzané, France

[5]UMR 5174 EDB (Laboratoire Évolution & Diversité Biologique), CNRS, Université Paul Sabatier, IRD, Toulouse, France

[6]CREAF, Cerdanyola del Vallès, Spain

[7]Sorbonne Université, CNRS, Station Biologique de Roscoff, UMR7144, Place Georges Teissier, Roscoff Cedex, France

[8]Université de Rennes 1, BOREA, Muséum National d'Histoire Naturelle, Sorbonne Université, Université de Caen Normandie, Université des Antilles, Campus de Beaulieu, Rennes, France

[9]France Energies Marines, Plouzané, France

[10]Department of Arctic and Marine Biology, UiT The Arctic University of Norway, Tromsø, Norway

[11]Centre d'Etudes Biologiques de Chizé, UMR 7372 du CNRS-La Rochelle Université, Villiers-en-Bois, France

Correspondence
Anthony Sturbois
Email: anthony.sturbois@espaces-naturels.fr

Funding information
Agence de l'eau Loire-Bretagne, Grant/Award Number: 180212501; European maritime and fisheries fund, Grant/Award Number: FEAMP 621-B; Institut Polaire Français Paul Emile Victor, Grant/Award Number: IPEV program N109; Ministre de la Transition Ecologique et Solidaire, Grant/Award Number: EJ N;2102930123; Office Français de la Biodiversit, Grant/Award Number: STABLELAKE SOLAKE; Région Bretagne, Grant/Award Number: OSIRIS PFEA621219CR0530023; Spanish Ministry of Economy, Grant/Award Number: CGL2017-89149-C2-2-R

Handling Editor: Aimeé T. Classen

Abstract

Ecologists working with stable isotopes have to deal with complex datasets including temporal and spatial replication, which makes the analysis and the representation of patterns of change challenging, especially at high resolution. Due to the lack of a commonly accepted conceptual framework in stable isotope ecology, the analysis and the graphical representation of stable isotope spatial and temporal dynamics of stable isotope value at the organism or community scale remained in the past often descriptive and qualitative, impeding the quantitative detection of relevant functional patterns. The recent community trajectory analysis (CTA) framework provides more explicit perspectives for the analysis and the visualization of ecological trajectories. Building on CTA, we developed the Stable Isotope Trajectory Analysis (SITA) framework, to analyze the geometric properties of stable isotope trajectories on n-dimensional ($n \geq 2$) spaces of analysis defined analogously to the traditional multivariate spaces (Ω) used in community ecology. This approach provides new perspectives into the quantitative analysis of spatio-temporal trajectories in stable isotope spaces (Ω_δ) and derived structural and functional dynamics

(Ω_γ space). SITA allows the calculation of a set of trajectory metrics, based on either trajectory distances or directions, and new graphical representation solutions, both easily performable in an R environment. Here, we illustrate the use of our approach by reanalyzing previously published datasets from marine, terrestrial, and freshwater ecosystems. We highlight the insights provided by this new analytic framework at the individual, population, community, and ecosystems levels, and discuss applications, limitations, and development potential.

KEYWORDS
changes, composition, dynamics, food web, functioning, spatial, stable isotope, structure, temporal, trajectories

INTRODUCTION

Stable isotope analysis has emerged as one of the most popular approaches to assess the trophic ecology of organisms (Fry, 2008), fluxes of matter and energy within and between ecosystems (Peterson & Fry, 1987), and animal movements (Bouillon et al., 2011; Rubenstein & Hobson, 2019). The quantitative analysis of stable isotope data is based on a large variety of available analytical tools ranging from qualitative inferences using isotopic niche (Newsome et al., 2007) to complex Bayesian mixing models that can be used to characterize food web structure and trophic pathways at multiple levels of biological organization (Layman et al., 2012). Understanding and quantifying spatial and temporal changes is an overarching topic in stable isotope ecology but studies are, to date, largely qualitative, and the development of quantitative approaches is needed.

The quantitative analysis of stable isotope dynamics in response to ecological and environmental changes, notably those induced by human activities, has been explored through the comparative analysis of temporal trajectories in a two-dimensional (usually $\delta^{13}C$ and $\delta^{15}N$) isotopic space (δ space). For instance, Schmidt et al. (2007) and Wantzen et al. (2002) quantified the direction and magnitude of temporal changes in food web structure based on the geometric properties of trajectories in the δ space. Schmidt et al. (2007) used specifically circular charts and statistics to represent and test direction shifts in the δ space. Turner et al. (2010) characterized attributes of path trajectories (size, direction, and shape) over data sets containing more than two temporal samples to provide a quantitative description of how stable isotope compositions change in response to spatial and temporal gradients, and tested their differences. Despite the fact that these works have provided substantial new perspectives notably for statistical and hypothesis testing, some limitations remain for the explicit quantitative description, analysis, and representation of the magnitude and the nature of changes in stable isotope composition.

In community ecology, several statistical frameworks have been proposed and used to test hypotheses on community dynamics (Buckley, Day, Lear, et al., 2021; De Cáceres et al., 2019). The dynamics of ecological communities has been traditionally represented on ordination diagrams in which changes over time are represented by a set of vectors linking consecutive ecological states (Austin, 1977; Hudson & Bouwman, 2007; Legendre & Salvat, 2015; Matthews et al., 2013). The geometric properties of trajectories, defined in the space of an ordination diagram, are considered as relevant parameters to quantify the dynamics of ecological systems. The potential of geometrically based methods was illustrated by De Cáceres et al. (2019) in the community trajectory analysis (CTA) framework. Compared with previous approaches based on ordination diagrams, De Cáceres et al. (2019) considered community dynamics as trajectories in a chosen space of community resemblance, with no limit in the number of dimensions included. In CTA, trajectories are defined as objects composed of consecutive segments to be analyzed and compared using distance- and direction-based metrics in the chosen multivariate space. Extending the initial framework, Sturbois, De Cáceres, et al. (2021) developed new CTA metrics and synthetic representation approaches, such as trajectory roses, and the inclusion of trajectory metrics in maps or ordination diagram.

By analogy to community ecology, the term and the concept of trajectory have been informally used in stable isotope ecology to characterize dynamics and represent them in spaces of analysis (either δ space, p-space sensu, Newsome et al., 2007; or spaces based on community-wide indices, e.g., Rigolet et al., 2015). The analysis and representation of stable isotope trajectories or contrasted patterns requires the use of quantitative geometric properties in 2D δ spaces often complemented by vectors in stable isotope scatter plots and/or circular representation (Agostinho et al., 2021; Black & Armbruster, 2021; Cucherousset et al., 2013; Schmidt et al., 2007). However, scientists are increasingly faced with multivariate datasets (i.e., >2 dimensions) in stable isotope ecology in

response to the potential use of (1) other isotopes to complement $\delta^{13}C$ and $\delta^{15}N$ (e.g., ^{34}S ([Connolly et al., 2004], δD [Doucett et al., 2007]) and (2) numerous structural and functional community-wide metrics or indices (Cucherousset & Villéger, 2015; Layman et al., 2007). While the availability of long-term, large-scale, and high-resolution data is one of the most limiting factors to study temporal patterns in stable isotope ecology, the development of methods to analyze, synthesize, and ultimately represent the dynamics of ecological systems still remains an essential issue to complete current approaches by more quantitative and formal explicit frameworks.

Building on CTA, we aim to provide a framework for the temporal analysis of stable isotope data at different levels of biological organization, from individuals to ecosystems to derive structural and functional trajectories in a new approach referred to as Stable Isotope Trajectory Analysis (SITA). We (1) provide a general definition of the trajectory concept applied in stable isotope ecology, adapted from CTA framework to stable isotope analysis, (2) present the package *ecotraj* designed for ecological trajectory analyses and here used specifically for SITA, and (3) illustrate potential applications of SITA using field, experimental or modeled data that include four main topics in stable isotope ecology: (i) individual and (ii) population levels, (iii) structural and functional trajectories of entire food webs, and (iv) modeling of stable isotope dynamics at high spatio-temporal resolutions.

TRAJECTORY CONCEPTS

Trajectory concept in stable isotope ecology

Founding works

Wantzen et al. (2002) and Schmidt et al. (2007) were the first to study directions and distances in δ spaces. Building on these works and the Adams and Collyer (2009) approach, Turner et al. (2010) provided a more explicit use of the concept of trajectory by the definition of trajectory attributes (size, direction, and shape). Despite the fact that Layman et al. (2012) recommended these geometrically based approaches in conjunction with area based in bivariate or multivariate isotopic space, to our knowledge, their use has currently been limited to bivariate spaces (e.g., $\delta^{13}C$-$\delta^{15}N$ biplots).

Conceptual definition

A trajectory in stable isotope ecology can be defined as a path in a chosen space of analysis, (Ω_δ or Ω_γ, depending whether the space is based on raw stable isotope data, or on derived indices, respectively), composed of one or different consecutive segments, resulting from repeated observations of a same sampling unit (individuals, populations, stations, food web, etc.). Observed temporal patterns can be characterized by distances and directions in Ω and used to define the nature (i.e., ecological meaning) and magnitude (i.e., importance) of temporal changes. The overall trajectory concept in stable isotope ecology can be adapted to different ecological questions, as illustrated in Section *Applications of SITA*.

Characterizing stable isotope trajectories

Formal definition of trajectory in stable isotope ecology

We follow here the CTA notation used by De Cáceres et al. (2019) to describe and compare trajectories in a multidimensional space of community composition. Given a target sample (individual, population, entire food web, station) whose dynamics is surveyed, let $o_1, o_2, ..., o_n$ be an ordered set of n observations ($n > 1$) and $t_1, t_2, ..., t_n$ the corresponding set of ordered survey times (i.e., $t_1 < t_2 < ... < t_n$). For all i in {1, 2, ..., n}, x_i contains the coordinates corresponding to o_i in a multidimensional space Ω. The geometry of the trajectory T is formalized using a set of $n - 1$ directed segments $\{s_1, ..., s_{n-1}\}$, where $s_i = \{x_i, x_{i+1}\}$ is a segment with endpoints (community states) x_i and x_{i+1}.

Definition of spaces supporting SITA

As for CTA, SITA requires the definition of Ω defined by the resemblance between pairs of observations, measured using a dissimilarity coefficient d. SITA is based on dissimilarity values contained in a distance matrix $\Delta = [d]$ (De Cáceres et al., 2019).

The trajectory concept in stable isotope ecology may be addressed in terms of stable isotope composition or food web structure and functioning involving similar attributes (i.e., trajectory metrics) but different data inputs and space of analysis.

Stable isotope Ω_δ space

Ω_δ is defined with stable isotope values of different elements. Coordinates in this space of analysis correspond to raw stable isotope data. Despite $\delta^{13}C$ and $\delta^{15}N$ being the most commonly used in a bidimensional context, other elements that are ecologically meaningful may also be considered for defining the Ω_δ space (e.g., hydrogen δD, sulfur $\delta^{34}S$, or oxygen $\delta^{18}O$). Coordinates in Ω_δ are used to compute the resemblance between ecological

states using d, where we suggest the adoption of the Euclidean distance, as it is commonly used in stable isotope ecology (Ben-David et al., 1997; Kline Jr. et al., 1993; Schmidt et al., 2007; Turner et al., 2010; Wantzen et al., 2002; Whitledge & Rabeni, 1997).

Structural and functional Ω_γ space

Looking for patterns in stable isotope ecology often leads to the calculation of community-wide metrics or any structural or functional indices based on raw stable isotope data (Cucherousset & Villéger, 2015; Layman et al., 2007; Rigolet et al., 2015). Ω_γ is defined with any indices derived from raw stable isotope data, used as ecological proxies, such as to characterize food web structure, and allow a comparison within and among systems.

Trajectory metrics

Metrics detailed in Section Trajectory metrics, here adapted for a stable isotope purpose in Ω_δ and Ω_γ, are part of the CTA framework (see De Cáceres et al. [2019] and Sturbois, De Cáceres, et al. [2021] for equations and more details). Note that additional metrics, not used here, are defined in these articles.

Distance-based metrics

Segment length (S). The trajectory segment length is the distance between two consecutive surveys (i.e., measurements). The length of a segment is given by the distance between its two endpoints. The greater the length of a trajectory segment, the greater is the distance between states. This metric is particularly relevant to analyze the magnitude and the variability of trophic trajectories and allows the distinction between gradual and abrupt changes.

Trajectory path length (L(T)). The trajectory path length is the sum of segment lengths for a given sampling unit. This metric informs about the overall temporal change.

Net change (NC). The net change is defined as the length between a pair of states, which includes a chosen baseline state (i.e., initial or reference state). When calculated at the scale of an overall study period or at the end level of a gradient, this metric evaluates the difference between the initial and the final state, that is, the overall net trajectory change.

Net Change Ratio (NCR). The net change ratio is defined as the ratio between the overall net trajectory change and the trajectory path length. A high *NCR* indicates that a great part of the trajectory path contributes to net changes and illustrates a relative consistency in the drivers of ecological dynamics. Inversely, a low NCR illustrates the versatility of these drivers and highlights that a small part of the trajectory path contributes to net changes.

Recovering or Departing Trajectory (RDT). Let us consider a triplet of states composed of baseline, intermediate, and final states. The dynamics with respect to the baseline state can be defined as recovering (i.e., return to the initial state) or departing (i.e., increasing distance from the initial state) by subtracting $NC_{\text{baseline to intermediate}}$ to $NC_{\text{intermediate to final}}$. $RDT > 0$ indicates a closer position at final state than intermediate state and consequently implies a recovering toward the initial state (RIS). Inversely, $RDT < 0$ indicates a farther ecological state at final than intermediate state and consequently implies a departure from the initial state (DIS).

Direction-based metrics

Angle Θ. Θ is the angle between two consecutive segments ordered in time measured on the Euclidean plane that contains the three states. The angle $0° < \Theta < 180°$ is defined as the change of direction in this plane. The trajectory is linear when $\Theta = 0°$. If $\Theta = 180°$, the trajectory is still linear but opposite in sense.

Angle ω. Instead of considering consecutive segments, angle ω allows the assessment of the linearity of changes with respect to a chosen reference segment (e.g., first segment) of an ecological trajectory.

When space Ω is 2D, ω (as well as Θ) can be reported in a 0–360° system, if needed.

Angle α. When space Ω_δ and Ω_γ is 2D, it becomes also relevant to consider trajectory segment directions with respect to the interpretation of the axes defining the space. Angle α is measured considering the second axis of the 2D diagram as the North (0°). α allows the comparison of segment direction with respect to the influence of the variables used to interpret the two axes. When Ω is an ordination space, users may calculate α if they decide that the variance is sufficiently explained by the first two axes of the ordination and can refer to the loadings of original variables or their degree of correlation with additional variables. In an Ω_δ space, α angles are a convenient way to express dynamics with respect to single isotope variability.

Directionality (DIR). The overall directionality of trajectories provides information about the consistency with which a sample follows the same direction and, therefore, the stability of ecological drivers that condition the stable

isotope trajectory. DIR is bounded between 0 and 1 where the maximum value corresponds to a straight trajectory (see equation 3 in De Cáceres et al., 2019).

Geometric resemblance between trajectories

De Cáceres et al. (2019) developed a geometrically based approach to trajectory resemblance that included the shape, size, direction, and position of trajectories with respect to the resemblance between all observations (state) belonging to a same trajectory. The approach defines resemblance between pairs of segments or overall trajectories and allows the centering trajectories to exclude differences in position, while keeping the other components of trajectory resemblance. Different distance are proposed and discussed to compute dissimilarity calculation depending of users interests (De Cáceres et al., 2019).

Representing trajectories in stable isotope ecology

The representation concepts provided here are valid for the representation of trajectories in both Ω_δ and Ω_γ spaces.

Trajectory diagrams

Temporal dynamics in stable isotope ecology are sometimes represented in 1D or 2D δ space by segment or arrows between consecutive surveys (Agostinho et al., 2021; Guzzo et al., 2011). Here, we propose a trajectory diagram (TD) concept to customize ordination diagrams by adding notably SITA metrics. Trajectory segments are normally represented by segments between surveys to form the trajectory path whose last segment is ended by an arrow. If one wants to go further in the representation of trajectory net changes, (1) net changes may be represented at each transitional state by the data point size and (2) the overall net change may be represented by a dotted line or arrow between the initial and final state of a time series. We recommend also the generalization of density curves in the periphery of trajectory diagrams, as is sometimes done to compare different food webs (Zapata-Hernández et al., 2021).

Trajectory rose diagram

Schmidt et al. (2007) first introduced the use of direction and distance in their arrow diagrams. Building on this approach, we propose a complementary use of the trajectory rose (TR) diagrams proposed by Sturbois, De Cáceres, et al. (2021) to represent stable isotope dynamics in a circular way. The TR diagram consists of a circular bar plot of angles ranging from 0° to 360°. The barplot structure of TR allows the presence of representing factors in different bar sections. Depending on the aim of the analysis, users can choose to represent the distribution of Θ, ω or α angles. Bars sizes represent the number of segments concerned by each range of direction (e.g., 15°) and cumulative segment length may be represented by a point at the head of each bar and colored according to length values (Sturbois et al., 2021). In $\delta^{13}C/\delta^{15}N$ Ω_δ space, angle α illustrates different stable isotope (SI) trajectory patterns according to increase and/or decrease in $\delta^{13}C$ and $\delta^{15}N$ values (0–90°: $+\delta^{13}C$ and $+\delta^{15}N$; 90–180°: $+\delta^{13}C$ and $-\delta^{15}N$; 180–270°: $-\delta^{13}C$ and $-\delta^{15}N$; 270–360°: $-\delta^{13}C$ and $+\delta^{15}N$). In Ω_γ space, directions distribution refers to structural and functional indices. Note that the TR diagram may be adapted if one wants to represent, with similar visually importance, both direction and distance (segment lengths or net changes instead of number of trajectory segments). In this case, the information of the TR becomes more similar to that of arrow diagrams (Schmidt et al., 2007).

Trajectory heat map

Stable isotope datasets with high temporal resolutions may require special representations as they can potentially saturate TD or TR diagrams.

Here, we propose the concept of a trajectory heat map (TH) to represent long-term SI dynamics. The heat map is a two-dimensional representation of data in which the changes in the distribution of a chosen trajectory metric over time are represented using cell colors (see Section *Spatio-temporal variability of $\delta^{13}C$ and $\delta^{15}N$ modeled isoscapes in the northeast Pacific*). TH allows the representation of the distribution of distance- and direction-based trajectory metrics.

If users aim to favor the representation of directions in TH, angles Θ, ω or α can be represented in a matrix of fixed cell size whose colors vary depending of the number of a given direction range occurring in a given period. As in the TR, we advise the use of any direction bin size (e.g., 15°) to provide a synthetic representation. The TH can be completed by peripheric bar plots to represent trajectory lengths involved in each direction range and period (see Section *Spatio-temporal variability of $\delta^{13}C$ and $\delta^{15}N$ modeled isoscapes in the northeast Pacific*). In 2D Ω_δ space, angle α illustrates, for example, different SI trajectory patterns according to respective increase and/or decrease of the two SI values (see Section *Direction-based metrics*). TH therefore provides a relevant

visual summary of complex data sets, highlighting the magnitude and the nature of SI dynamics (TH cells clustering, barplots). In the TH concept, users can easily choose to represent the distribution of segment lengths or any trajectory metrics with respect to time, depending on ecological questions.

Trajectory maps

Expanding Sturbois, De Cáceres, et al. (2021), we propose the use of trajectory metrics as trajectory map (TM) input for the representation of temporal patterns in sampling units on geographic coordinates. Two examples are included here to illustrate the potential of the TM concept.

Trajectory map from initial state

We suggest the adaptation of the TM concept proposed by Sturbois, De Cáceres, et al. (2021) to represent site scale dynamics in Ω_δ or Ω_γ through geometrical properties of trajectories in synthetic figures accounting for temporal variability at the spatial unit scale. The use of a single map is proposed to represent all at once for each site of a study area (see Section *Biological invasions and trophic structure dynamics of lake fish communities*): (1) net change between x_1 and $x_{n\text{-survey}}$, (2) segment length (or subtrajectory length) $S_{i>1}$, and $S_{j>i}$, and (3) RIS or DIS segment or subtrajectory lengths between x_i and $x_{n\text{-survey}}$. Net changes are represented through a circular symbol proportional to the length to vector x_1-$x_{j>i}$. On both sides, a bottom triangle symbol represents the x_1-$x_{i>1}$ vector and a top triangle the $x_{i>1}$-$x_{j>i}$ vector. For both triangles, the size is proportional to the length of respective vectors, while the orientation and color of the top triangle illustrate the direction (recovering or departing) of the second vector with respect to the initial or baseline state.

Isoscape trajectory map

The spatial distribution of SI in environmental materials can be predicted, using models of isotope-fractionating processes and data describing environmental conditions, and represented through isotopic landscape, called isoscapes (Bowen, 2010; West et al., 2008). We adapted the TM concept for isoscape datasets characterized by high spatial resolutions and a minimum of two temporal surveys or modeling. This particular concept of TM is inspired by wind/current map where the magnitude and the direction of wind/current are represented through multiple vector covering large areas. In the isoscape TM (ITM), the direction of arrows represents angle α in a 2D Ω_δ space (e.g., $\delta^{13}C/\delta^{15}N$), and size illustrates trajectory length (see Section *Spatio-temporal variability of $\delta^{13}C$ and $\delta^{15}N$ modeled isoscapes in the northeast Pacific*). The representation of trajectory length is improved by a color raster of spatially interpolated length values.

SOFTWARE AVAILABILITY

In 2019, De Cáceres and colleagues proposed the CTA framework and functions for the calculation of associated metrics. These functions were included in package *vegclust*. In 2021, Sturbois et al. extended the CTA framework with new metrics and figure concepts. New functions were added in package *vegclust*. The present article goes further in the adaptation of CTA, bridging a gap identified in the consideration of dynamics in SI ecology, and starting the exploration of trajectory analysis beyond the sites × species matrix. All these recent developments, and the fact that trajectory analysis can be applied to different spaces, claimed a new package specifically devoted to ecological trajectory analysis that would allow taxonomic, functional or SI trajectory analyses within the same tool through complementary space of analysis (Ω).

The package *ecotraj* (De Cáceres [2019], Sturbois, De Cáceres, et al. [2021]) assists ecologists in the analysis of temporal changes of ecosystems, defined as trajectories on a chosen multivariate space, by providing a set of trajectory metrics and visual representations. It includes functions to perform trajectory plots and to calculate the set of distance and direction-based metrics (length, directionality, angles, etc.) as well as metrics to relate pairs of trajectories (dissimilarity and convergence). Currently, Trajectory analysis (SITA as well as CTA) can be performed using the "ecotraj" functions available on CRAN and GitHub repositories (https://emf-creaf.github.io/ecotraj/index.html). R codes to create figures are also shared to facilitate the use and the customization of our trajectory chart concepts (Data S1) and a new vignette has been added in the documentation of the package.

APPLICATIONS OF SITA

Six ecological applications (EA) were chosen to illustrate the use of SITA metrics and representation concepts for stable isotope dynamics within different ecological systems and to answer various ecological questions (Figure 1): stable isotope trajectories at the (1) individual (EA1 and EA2) and (2) population (EA1, EA3 and EA4) levels, (3) structural and functional trajectories at the scale of entire food webs (EA4 and EA5), and (4) stable isotope dynamics at high spatio-temporal resolutions (EA6).

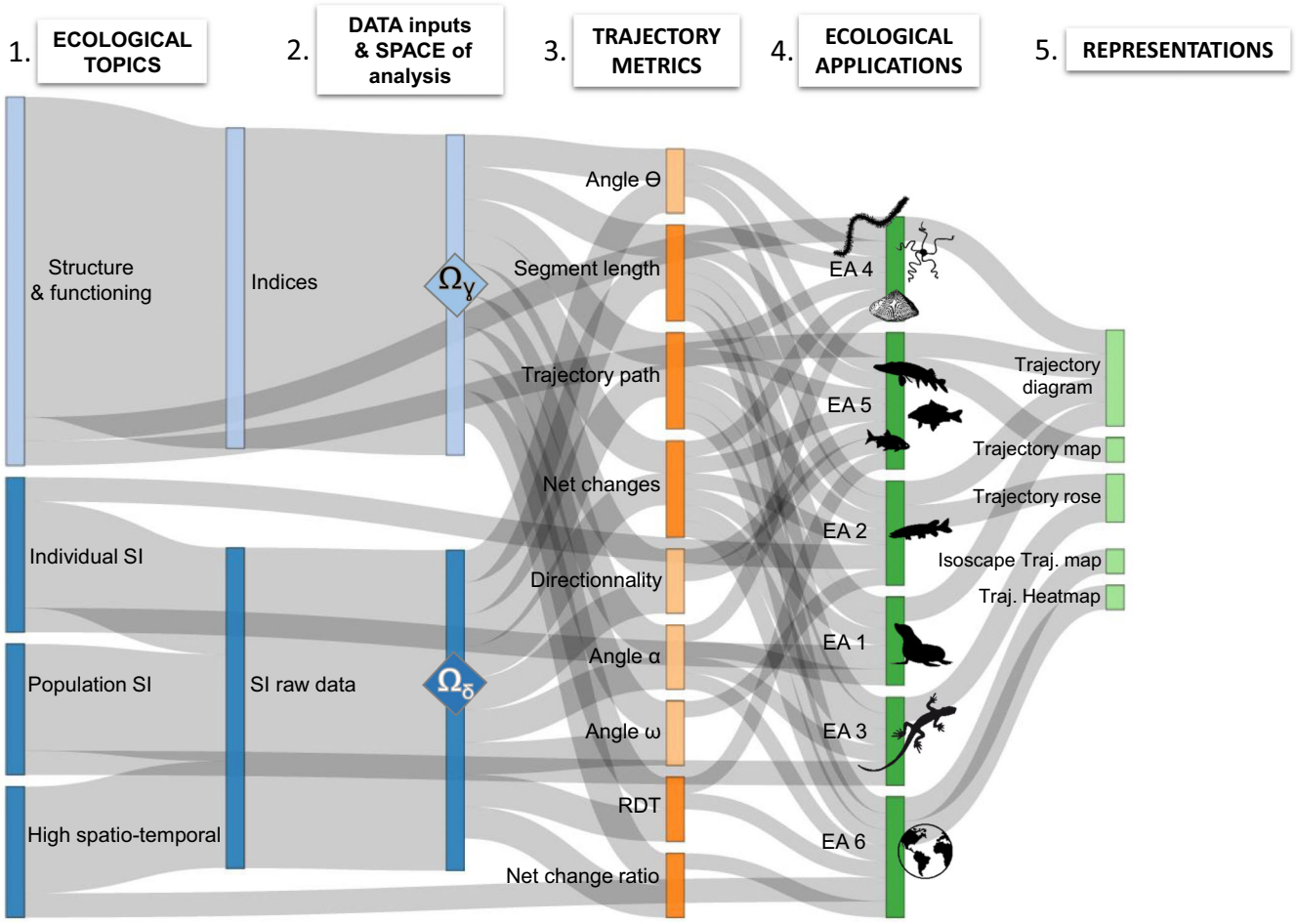

FIGURE 1 Levels of analysis and ecological questions drive input data used to define the space of analysis supporting SITA. While structural and functional analysis requires community-wide metrics or indices to define Ω_{γ}, raw stable isotope data are used for the definition of Ω_{δ} that supports stable isotope trajectories at different levels from individual to population, or for ecological questions that involve high stable isotope spatio-temporal resolutions. The SITA adaptability allows the calculation of distance- and direction-based trajectory metrics in both, Ω_{δ} and Ω_{γ}, and their visualization in different figures devoted to the representation of dynamics

Spatial and temporal resource partitioning in fur seals

Context

Many generalist populations are composed of individual specialists and individual specializations are increasingly recognized as an important component of many ecological and evolutionary processes (Bolnick et al., 2003), making crucial testing the consistency of individual specialization.

Methods

$\delta^{13}C$ and $\delta^{15}N$ values of metabolically inert tissues reflect diet at the time of their growth, and continuously growing tissues can be used as time-recorders of the movement and dietary history of individuals. Fur seals (the Antarctic fur seal *Arctocephalus gazella* [AFS] and sub-Antarctic fur seal *A. tropicalis* [SAFS]) whisker SI values yielded unique long-term information on individual behavior that integrated the spatial, trophic, and temporal dimensions of the ecological niche (Cherel et al., 2009; Kernaléguen et al., 2012). The foraging strategies of these two species of sympatric fur seals were examined in the 2001/2002 winter at Crozet, Amsterdam, and Kerguelen islands (Southern Indian Ocean) by measuring the SI compositions of serially sampled whiskers (see Kernaléguen et al., 2012, 2015 for SI preparation and analyses). The method consists of the analysis of consecutive whisker sections (3-mm long) starting from the proximal (facial) end, with the most recently synthesized tissue remaining under the skin. Only individuals ($n = 47$) with whiskers totaling at least 30 sections were selected, and only those 30 sections were considered here (Sturbois, Cucherousset, et al., 2021a), from t_1 (more recent values) to t_{30} (oldest values). SITA was performed to track individual specialization within and among four fur seal populations. Different metrics (segments lengths, trajectory

TABLE 1 Characteristics of fur seal trajectory clusters: number of individuals (n), stable isotopes (SI), distance-based metrics, number of individuals depending of species and genders (female *A. gazella* [FAFS], male *A. gazella* [MAFS], female *A. tropicalis* [FSAFS], male *A. tropicalis* [MSAFS]) and breeding sites (Crozet [Cro], Kerguelen [Ker], Amsterdam [Am]). Values are means ± SE. Data sets from Kernaléguen et al. (2012)

		Whisker SI values		Distance-based SITA metrics			n/species-genders				n/breeding places		
Clusters	n	$\delta^{13}C$ ‰	$\delta^{15}N$ ‰	**Trajectory path**	**Segment length**	**Net changes**	**FAFS**	**MAFS**	**FSAFS**	**MSAFS**	**Cro**	**Ker**	**Am**
1	2	−22.29 ± 0.17	9.77 ± 0.20	21.77 ± 6.14	1.50 ± 0.21	3.86 ± 0.51		2			2		
2	19	−17.54 ± 0.04	10.52 ± 0.02	14.59 ± 0.99	0.99 ± 0.03	1.79 ± 0.09	15	1	3		13	6	
3	6	−16.65 ± 0.07	11.93 ± 0.07	19.61 ± 1.01	1.33 ± 0.03	2.70 ± 0.11		2		4	6		
4	4	−18.96 ± 0.23	11.39 ± 0.14	35.22 ± 3.51	2.36 ± 0.12	6.53 ± 0.24		4			4		
5	6	−16.57 ± 0.03	10.79 ± 0.03	9.39 ± 0.80	0.64 ± 0.03	1.21 ± 0.09			5	1	6		
6	10	−15.42 ± 0.02	13.32 ± 0.04	12.54 ± 0.55	0.84 ± 0.02	1.59 ± 0.06			10				10
Total	**47**						**15**	**9**	**18**	**5**	**31**	**6**	**10**

path, net changes, angle α) were calculated in the 2D Ω_δ space ($\delta^{13}C/\delta^{15}N$) for each individual. Dissimilarities between individual trajectories were calculated (directed segment path dissimilarity; De Cáceres et al., 2019), and was used with the resulting symmetric matrix as input in a hierarchical cluster analysis (ward.D2 clustering method), to define different groups of similar individual trajectories. Segment length, trajectory path length, and whisker $\delta^{13}C/\delta^{15}N$ values were summarized to illustrate the trophic variability for each trajectory cluster. Hermans–Rasson and Watson–William tests were performed to test the homogeneity of angle distribution among trajectory within each cluster and the difference of segment direction between clusters. SITA metrics were represented in trajectory diagrams and a trophic TR.

Results

SITA revealed contrasted stable isotope dynamics among species, sexes, and individuals. Hierarchical cluster analysis identified six main trajectory clusters, characterized by differences in SITA metrics and whisker $\delta^{13}C/\delta^{15}N$ values (Table 1 and Figure 2). Clusters 1, 3, and 4 were exclusively composed of trajectories corresponding to males, from AFS only (clusters 1 and 4) or from both species (cluster 3). These clusters were characterized by the highest values in distance-based metrics, revealing wider foraging strategies (Table 1). Clusters 1 and 4 were characterized by lower $\delta^{13}C$ values contrasting with cluster 3. Cluster 2, characterized by a lower isotopic variability, grouped all of the 15 AFS females from Crozet and Kerguelen and included also one AFS male and three SAFS females. Individuals in cluster 5 (five females and one

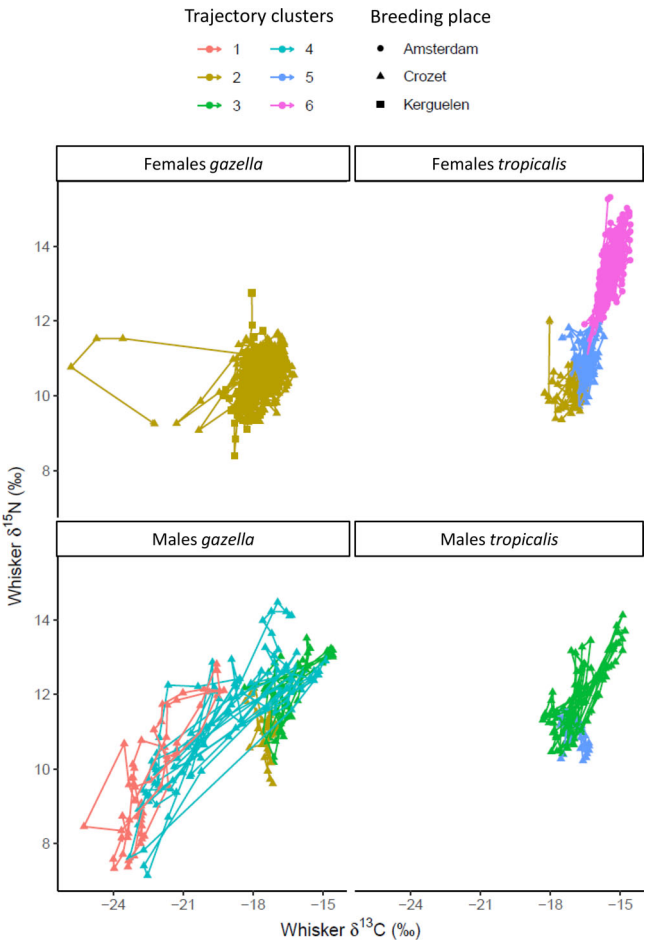

FIGURE 2 Individual fur seal trophic trajectories for males and females of *A. gazella* and *A. tropicalis*. Arrows connect all whiskers section stable isotope values from t_1 to t_{30} (i.e., most recent to oldest stable isotope values). Colors correspond to trajectory clusters and shapes to breeding sites. Data from Kernaléguen et al. (2012)

male SAFS from Crozet) exhibited the lowest isotopic variability. Cluster 6 was exclusively composed of SAFS females from Amsterdam, revealing a clear trophic segregation of females breeding there.

Different foraging strategies characterized by some overlaps, and partly influenced by breeding sites (Figure 2), were revealed for AFS males (distributed in four trajectory clusters) and SAFS females (three clusters). The time series of net changes (Figure 3, Table 1) revealed that each individual exhibited a more or less well defined trophic cycle whose amplitude and period depended on trajectory clusters. The distribution of trajectory segment directions (α angles) was heterogeneous for five of the six clusters (Herman–Rasson tests, $p > 0.05$) and some differences also existed among clusters (Figure 4).

Discussion

The estimated $\delta^{13}C$ values of the Polar Front and of the Subtropical Front for fur seal whiskers were approximately −19 and −16‰, respectively (Cherel et al., 2009). Accordingly, Kernaléguen et al. (2015, 2012) showed (1) a spatial foraging gradient from southern cold waters to northern and warmer areas for, in the order, AFS male, AFS female and SAFS male and female, (2) male benthic feeding strategy near breeding places, and (3) $\delta^{13}C$ and $\delta^{15}N$ oscillation patterns in most whiskers. Trajectory analysis results were congruent with those conclusions, but we went further showing that individual feeding strategies transcend preestablished categories such as species, genders, and breeding places, which was not primarily evident from analysis at the population level. This application confirms that SITA metrics and representations are relevant to track the shape and the magnitude of stable isotope trajectories in δ space, at different scales, from individual to population, and particularly to reveal subtle relevant functional patterns in spatio-temporal resource partitioning.

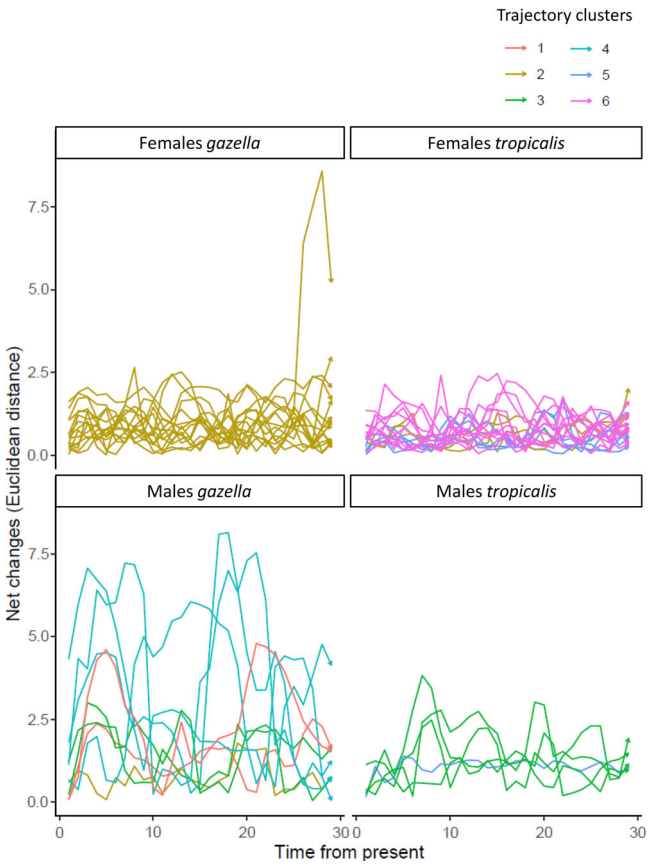

FIGURE 3 Fur seal individual trophic trajectories. Net change time series for males and females of both AFS and SAFS. Arrows connect all whiskers section stable isotope values from t_1 to t_{30} (i.e., most recent to oldest stable isotope values). Colors correspond to trajectory clusters. Data from Kernaléguen et al. (2012)

Ontogenic stable isotope trajectories of juvenile fish

Context

Intraspecific variability has strong ecological implications across levels of biological organization and can modulate the outcomes of individual life history. This is particularly true for movement along habitats, which is an ubiquitous phenomenon with important consequences on individuals.

Methods

Cucherousset et al. (2013) released 192 individually tagged, hatchery-raised, juvenile pike (*Esox lucius* L.) with variable body size and initial trophic position (fin $\delta^{13}C/\delta^{15}N$ values). Based on $\delta^{15}N$ values, individuals were classified into zooplanktivorous ($\delta^{15}N < 10$‰) and piscivorous ($\delta^{15}N > 10$‰), as cannibalism is commonly observed in this species. Individuals were released in a temporarily flooded grassland (FG) where pike eggs usually hatch in the Brière marsh (France) to identify the determinants of juvenile natal departure. The release site was connected through a unique point to an adjacent pond (AP) used as a nursery habitat. The pond strongly differs from the FG in many ecological features such as food availability (zooplankton and fish prey). Fish were continuously recaptured when migrating from the FG to the AP. Recaptured individuals ($n = 29$) were anesthetized, checked for tags, measured for fork length,

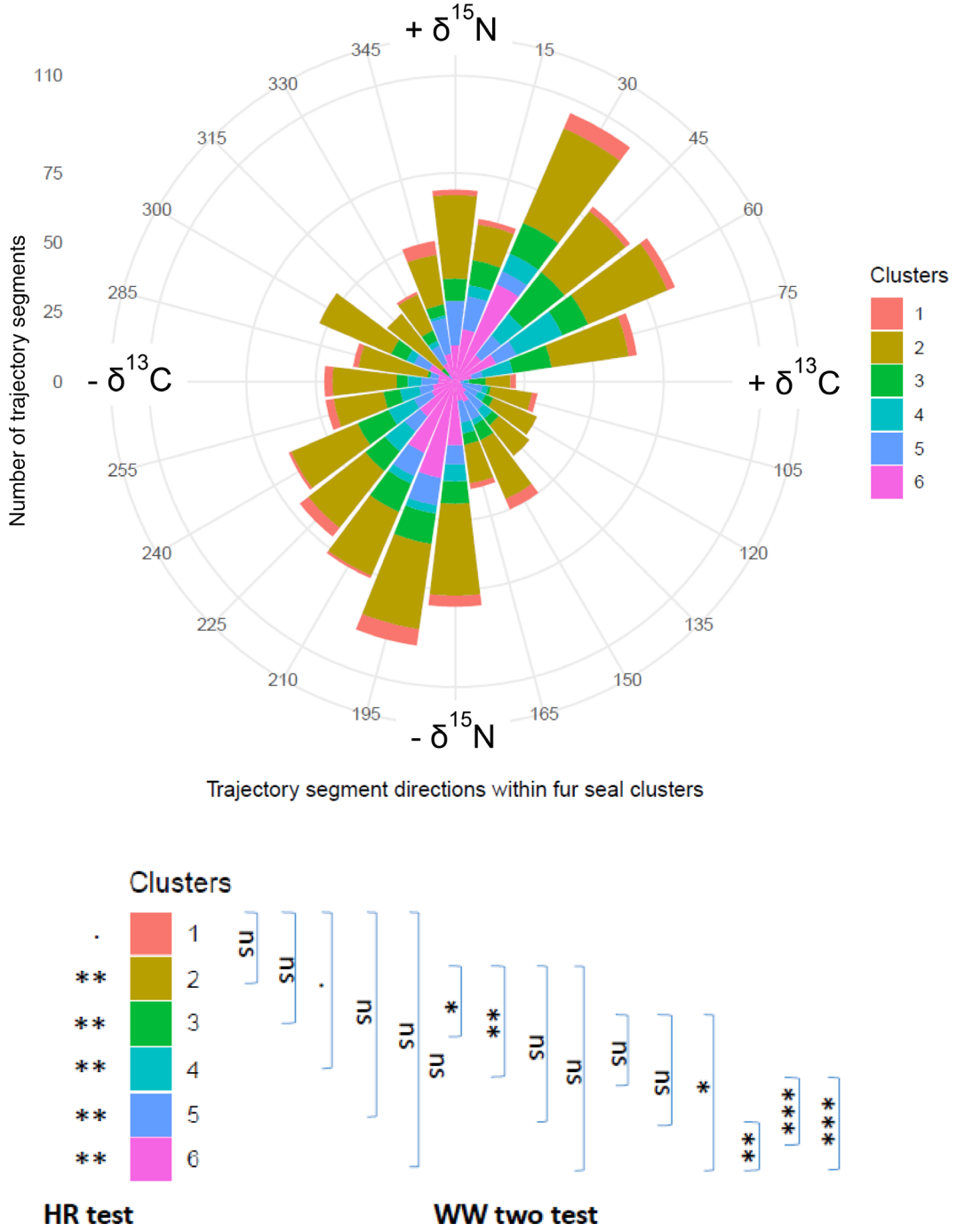

FIGURE 4 Angle α trajectory roses of fur seals trajectory cluster. Angle α was calculated in 2D Ω_δ space ($\delta^{13}C/\delta^{15}N$) and represented by range (15°) of direction. Bar size represents the number of trajectory segments (all individual within each trajectory clusters). Watson–William (WW) two test and Herman–Rasson (HR) test were used to test the difference between cluster and the uniformity of directions, respectively. (*p*-values: >0.05; * <0.05; ** < 0.01; < 0.001). Data from Kernaléguen et al. (2012)

fin-clipped to quantify changes in $\delta^{13}C$ and $\delta^{15}N$ values (Sturbois, Cucherousset, et al., 2021a), and released. Net changes and angle α were calculated in Ω_δ, and followed by hierarchical clustering of trajectories, as explained for the previous example.

Results

Overall, released individuals exhibited lower $\delta^{13}C$ (−2.49 ‰ ±0.82, mean ± SD) and $\delta^{15}N$ (−1.46 ‰ ± 0.89) when recaptured. The hierarchical cluster analysis

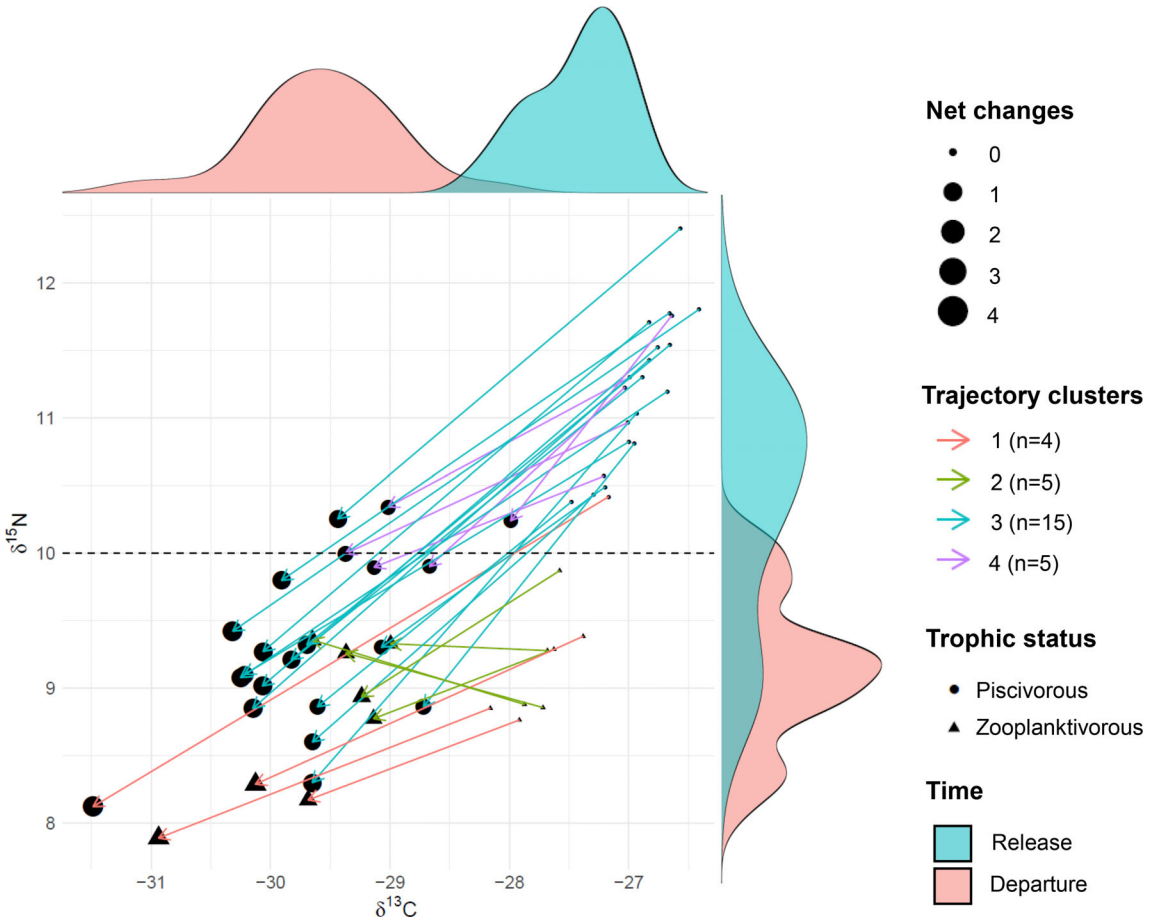

FIGURE 5 Trajectory diagram of pike released in a flooded grassland and recaptured when emigrating into an adjacent pond. Arrows represent the trajectory path for each pit-tagged individual. Colors correspond to trajectory clusters. Density curves at the periphery of the trajectory diagram represent the distribution of all samples according to $\delta^{13}C$ (x) and $\delta^{15}N$ (y), and capture (green = release; red = departure). The dashed line separates piscivorous from zooplanktivorous individuals (zooplanktivorous [$\delta^{15}N < 10‰$] vs. piscivorous [$\delta^{15}N > 10‰$]). Data from Cucherousset et al. (2013)

TABLE 2 Characteristics of pike trajectory clusters: number of individuals (n), residence time in flooded grassland (Res. time), size shift (mm), growth rate (mm day^{-1}), SI shift, SITA metrics, trophic status at release (zooplanktivorous [$\delta^{15}N < 10$] vs. piscivorous [$\delta^{15}N > 10$]). Values are means ± SE (±SD for total). Data sets from Cucherousset et al. (2013)

					SI shifts		SITA metrics		Trophic status	
Clusters	***n***	**Res. time**	**Size shift**	**Growth rate**	**$\delta^{13}C$ ‰**	**$\delta^{15}N$ ‰**	**Net changes**	**Angle *α***	**Zplankt.**	**Pisciv.**
1	4	18.50 ± 0.87	35.25 ± 1.44	1.90 ± 0.38	−2.90 ± 0.20	−1.24 ± 0.14	3.16 ± 0.63	248.14 ± 2.17	3	1
2	5	18.20 ± 0.86	34.40 ± 0.71	1.90 ± 0.23	−1.58 ± 0.03	−0.10 ± 0.11	1.67 ± 0.10	266.57 ± 8.89	5	
3	15	13.67 ± 1.42	26.13 ± 4.78	1.91 ± 0.10	−2.90 ± 0.28	−2.10 ± 0.19	3.13 ± 0.26	233.92 ± 1.35		15
4	5	9.60 ± 1.21	18.20 ± 1.71	1.96 ± 0.18	−1.86 ± 0.17	−1.09 ± 0.15	2.63 ± 0.42	239.12 ± 5.53		5
Total	**29**	**14.41 ± 5.14**	**27.45 ± 10.06**	**1.92 ± 0.27**	**−2.49 ± 0.82**	**−1.46 ± 0.89**	**2.95 ± 1.02**	**242.41 ± 15.60**	**8**	**21**

performed on pike trajectory dissimilarities matrix between release at FG and departure to AP separated four main trajectory clusters (Figure 5 and Table 2). Clusters 1 and 2 grouped mostly zooplanktivorous individuals at release, characterized by late emigration to the pond (18.50 ± 0.87 and 18.20 ± 0.86 days, mean ± SE). Cluster 1 was characterized by higher net changes (3.16 ± 0.63) and more uniform direction (248.14° ± 2.17) than cluster 1 (1.67 ± 0.10; 266.57° ± 8.89). Clusters 3 and 4 grouped initially piscivorous individuals. High $\delta^{15}N$ values for most

individuals at emigration suggested either that these individuals kept feeding at higher trophic levels than individuals from clusters 1 and 2, or a post-release period in the FG not long enough to reach the isotopic equilibrium. Difference in residence time (i.e., 13.67 ± 1.4 and 9.60 ± 1.2 for clusters 3 and 4 respectively) was responsible for the difference in $\delta^{15}N$ values between these two clusters (i.e., there was less time for hatchery SI values of cluster 3 to be diluted in FG stable isotope values). Among all clusters, the growth rate was very similar (1.92 ± 0.27 mm·day^{-1}).

Discussion

Results obtained using SITA confirm the initial findings and interpretation in Cucherousset et al. (2013) but also provided additional information. The cluster analysis of trajectory dissimilarity allowed an efficient discrimination of trajectory patterns. Although these patterns were briefly discussed in the initial study, we were able to define trajectory and SI properties in the four clusters, which clearly separated different ontogenic strategies among released individuals. Furthermore, the use of the TD offered a more complete representation of (1) trajectories properties at the population level (density curves), and (2) clusters and individuals levels (individual trajectory paths).

Trophic consequences of experimental warming on lizards

Context

Climate change is an important facet of ongoing environmental changes induced by human activities. While there is an increasing knowledge of how species will respond to climate changes in term of distribution, our ability to understand and predict changes in biotic interactions, such as predator–prey dynamics, is limited.

Methods

Bestion et al. (2019a) experimentally quantified the consequences of a 2°C warming on the trophic niche of a generalist lizard predator (*Zootoca vivipara*). Climate was manipulated in a 10 × 10 m enclosure with similar natural vegetation and invertebrate communities, and a wide variety of thermal microhabitats (dense vegetation, rocks and logs, ponds; see Bestion et al. [2019a] for more details). In June 2013, individuals belonging to two life stages (juveniles and adults) and from both sexes were allocated at similar density to 10 enclosures: five enclosures with a "present-day climate" and five enclosures with a "warm climate," that is, 2°C warmer on average. There was no difference in $\delta^{13}C$ and $\delta^{15}N$ values between treatments at the start of the experiment. In mid-September 2013, surviving lizards were recaptured and a tail tip was collected for SI analysis. Because SI values of trophic resources varied among enclosures, a baseline correction ($\delta^{13}C_{cor}$ and $\delta^{15}N_{cor}$) was performed to allow between-treatment comparisons (Bestion et al., 2019a, 2019b). Enclosures from the two treatments were paired in five blocks (A–E used as replicates), and used to characterize, respectively, the initial (present-day climate) and final (warmer climate) states of a one-segment trajectory for five paired lizard populations in response to warming. Because the analysis focused particularly on shifts rather than absolute SI values, we favored the representation of net change and angle α, calculated in Ω_δ, in TR.

Results

Some differences in the magnitude of trajectories were observed among pairs of enclosures (Figure 6). Block C was characterized by the highest net change (1.63 ± 0.19) for all individuals (adults and juveniles of both sexes), whereas shifts in SI values in response to warming were more limited in other blocks (A: 0.36 ± 0.15; B: 0.39 ± 0.36; D: 0.55 ± 0.44; E: 0.47 ± 0.21‰). Some differences were also observed within paired enclosures where net changes were contrasted between individuals. For instance, in block D, adult males displayed the highest response (1.12), whereas juvenile females displayed the lowest response (0.12). Differences were also observed in the direction of the trajectories (Figure 6). In block C, all individuals displayed similar directional changes (10.23 ± 3.88°) with trajectories mainly implying increase in $\delta^{15}N_{cor}$ values and limited $\delta^{13}C_{cor}$ shifts. The other blocks displayed more variable responses to warming. For example, individuals from block A exhibited different directions in Ω_δ, revealing different patterns of SI changes.

Discussion

Using conventional statistical analyses, Bestion et al. (2019a) concluded that lizards from warmer conditions had higher $\delta^{15}N_{cor}$ values, whereas nonsignificant changes in $\delta^{13}C_{cor}$ values were observed. By pairing enclosures for trajectory analysis, SITA results were in accordance with these findings, but they also highlighted the existence, in some cases, of other responses to warming, with approximately

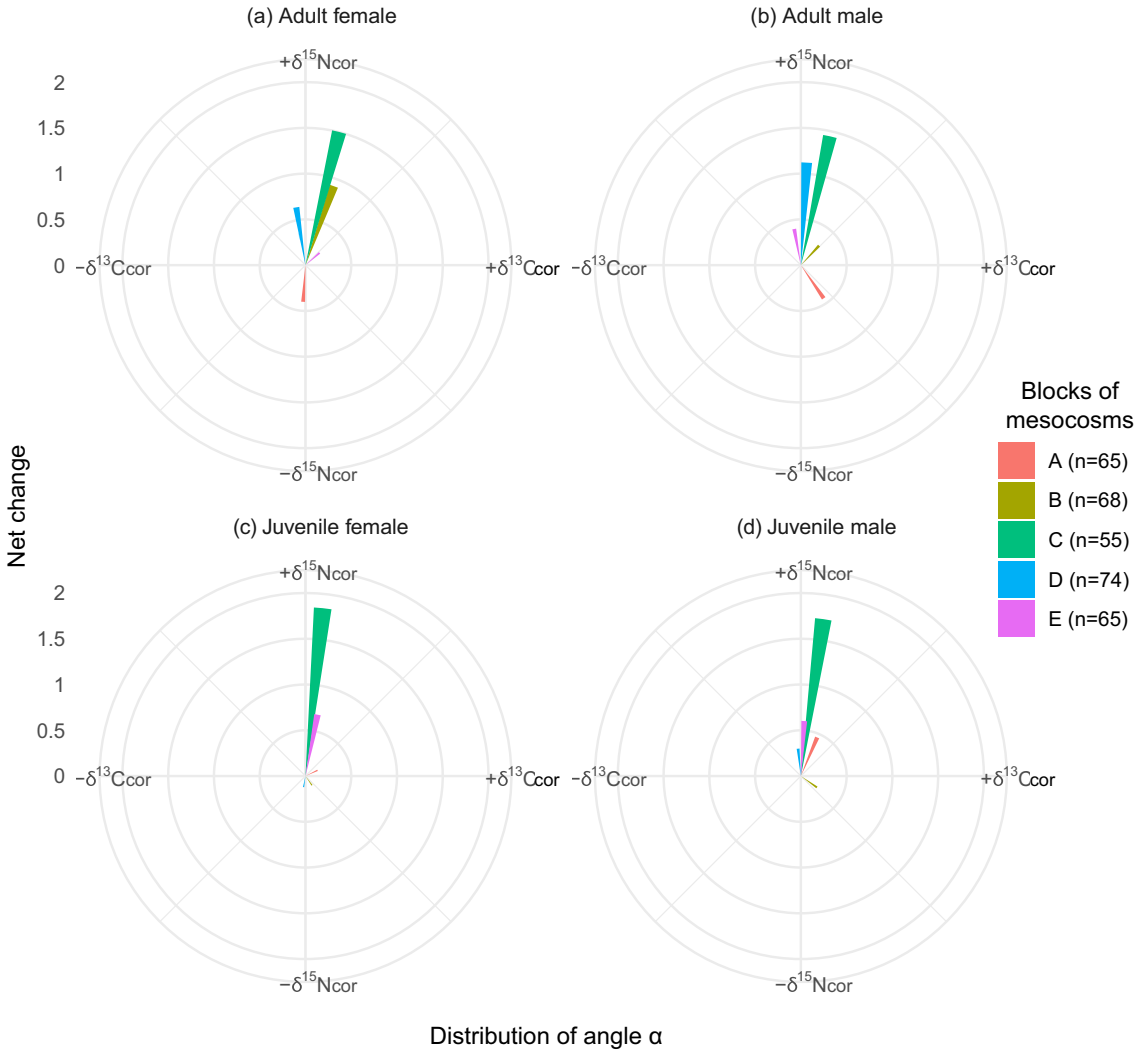

FIGURE 6 Angle α trajectory roses for each lizard life stage/sex categories within each block of enclosures (warming between present day and warm treatments). Angle α was calculated in 2D Ω_δ space ($\delta^{13}C_{cor}$ and $\delta^{15}N_{cor}$). Bar size represents the net change for each enclosure block (colors) and each life stage/sex (a: adult females; b: adult males; c: juvenile females; d: juvenile males). Data from Bestion et al. (2019b)

25% of all individuals (life stage, sex and blocks) displaying slight decreases in $\delta^{13}C_{cor}$ and $\delta^{15}N_{cor}$ values. These findings may reveal some additional context dependency in the response to warming observed at the individual level.

Contrasted trajectories in pristine and impacted sandy beaches undergoing green tide events

Context

Excess nutrient inputs is one of the most important human-induced pressures in freshwater and marine water bodies. The assessment of the consequences of the resulting eutrophication on ecosystems functioning is necessary to identify and describe disturbance pattern, especially in comparison with unperturbed habitat.

Methods

Quillien et al. (2016) studied changes in sandy beach (SB) food web structure and functioning in response to green algae proliferation during green tide (GT) events. Fieldwork was conducted seasonally in the bay of Douarnenez (Brittany, France) in May, July, September and November 2012 at two SB: one impacted by GT events and the other under pristine conditions (No_GT). Sampling and laboratory steps performed for community and SI analyses were described in Quillien et al. (2016). Trophic trajectories in pristine and impacted SB were analyzed both at the food

web (1) and basal source/centroid/population (2) levels. At the food web level, functional diversity indices (Villéger et al., 2008) were calculated in the SI space (Sturbois, Cucherousset, et al., 2021a) as proposed by Cucherousset and Villéger (2015) and Rigolet et al. (2015): Isotopic functional richness (IFRic), evenness (IFEve) and divergence (IDFiv). Mean distance to nearest neighbor (MNN) and centroid (MDC) were also calculated. Patterns of biomass were assessed by weighting SI values of every species prior to indices calculations. A principal component analysis (PCA), followed by SITA was performed on trophic indices (Ω_γ) to analyze changes in food webs properties at pristine and impacted SB over time. Distance (segment length, net changes) and direction-based metrics (DIR, angle Θ) were calculated. SITA was complementarily performed in Ω_δ defined with $\delta^{13}C$ and $\delta^{15}N$ values (Sturbois, Cucherousset, et al., 2021a) for basal sources and food web centroids. Distance-based metrics were calculated and trajectories at the different levels were represented in trajectory diagrams.

Results: Structural and functional trajectories

The pristine SB was characterized by a lower structural and functional temporal variability (trajectory path = 6.09, mean segment length = 2.33 ± 0.48) than impacted SB (16.13, 5.38 ± 1.46) (Figure 7). Low DIR indicated non-straightforward trajectories for both sites (No_GT = 0.45 vs. GT = 0.33). Considering the first two Ω_γ dimensions, responsible for 92% of the total variance, the first trajectory segments (i.e., between May and July) were quite similar in direction for both sites (angle α: No_GT = 89.06° vs. GT = 69.07°) but different in magnitude (S1 length: No_GT = 2.29 vs. GT = 5.43), therefore highlighting similar trends of index values, except for IFDiv (Figure 7). For GT SB, S1 and S2 were followed by a directional rupture in Ω_γ ($\Theta_1 = 107.00°$; $\Theta_2 = 133.14°$) implying contrasted functional and structural shifts. At No_GT SB, S2 followed a more straightforward path, whereas S3 was characterized by an important direction change ($\Theta_1 = 34.03°$; $\Theta_2 = 138.90°$). At the scale of the overall study period, structural and functional variability was higher in SB harboring GT (NC = 4.74) than in pristine SB (NC = 3.30). Between May and November, pristine SB was characterized by positive shifts in IFRic, and MDC and MNN, and negative shifts in IF Eve and IFDiv. At GT SB, IFDiv and IFRic were characterized by a moderate increase, whereas MNN, IFEve, and MDC decreased. At the scale of each trajectory segment, No_GT SB was mainly characterized by shifts in IFRic values, whereas GT SB was typified by highest magnitudes of changes and contrasted shifts. Specifically, the decrease in MDC and MNN values occurring between July and September started to recover in November.

Sources/centroid-specific trajectories in the $\delta^{13}C$ and $\delta^{15}N$ space

Basal sources trajectories were longer, therefore highlighting a high variability in SI values (Figure 8). Whereas particulate organic matter (POM) in impacted and pristine beaches exhibited similar trajectory length (6.67 vs. 5.99), sedimentary organic matter (SOM) was characterized by a lower variability where GT occurred (3.66 vs. 6.05). *Ulva* spp. was characterized by the highest SI variability (8.56). Specifically, POM trajectories at both sites were similar in terms of nature, seemingly cyclic, but different in magnitude. SOM at both sites depicted more complex trajectories, with similar but not synchronized SI trends, notably in September and November (i.e., November SOM No_GT vs. September SOM GT, and inversely). Trajectories of centroids did not reflect the magnitude of basal sources dynamics in GT (trajectory path = 1.40, net change = 0.76) and No_GT SB (1.62, 0.53). Trajectories of basal sources and centroid highlighted a constant enrichment in ^{13}C, except for SOM in September, while $\delta^{15}N$ patterns were less obvious.

Discussion

Results were congruent with the conclusions of Quillien et al. (2016) that showed a simplification of food web structure and functioning in the SB where the GT tide occurred. The consideration of SI dynamics at basal sources and centroids levels helps to better understand structural and functional trajectories at both sites. The interest in SITA was due to the consideration of both sites through their own dynamics exhibited at different levels. Specifically, SITA pointed out (1) low differences and variability of food web centroids at both beaches, and (2) contrasted structural and functional trajectories depicting the initiation of two potential food web cycles, which differed in nature and magnitude.

Biological invasions and trophic structure dynamics of lake fish communities

Context

Community assembly can strongly impact the dynamics of biological diversity and the functioning of ecosystems

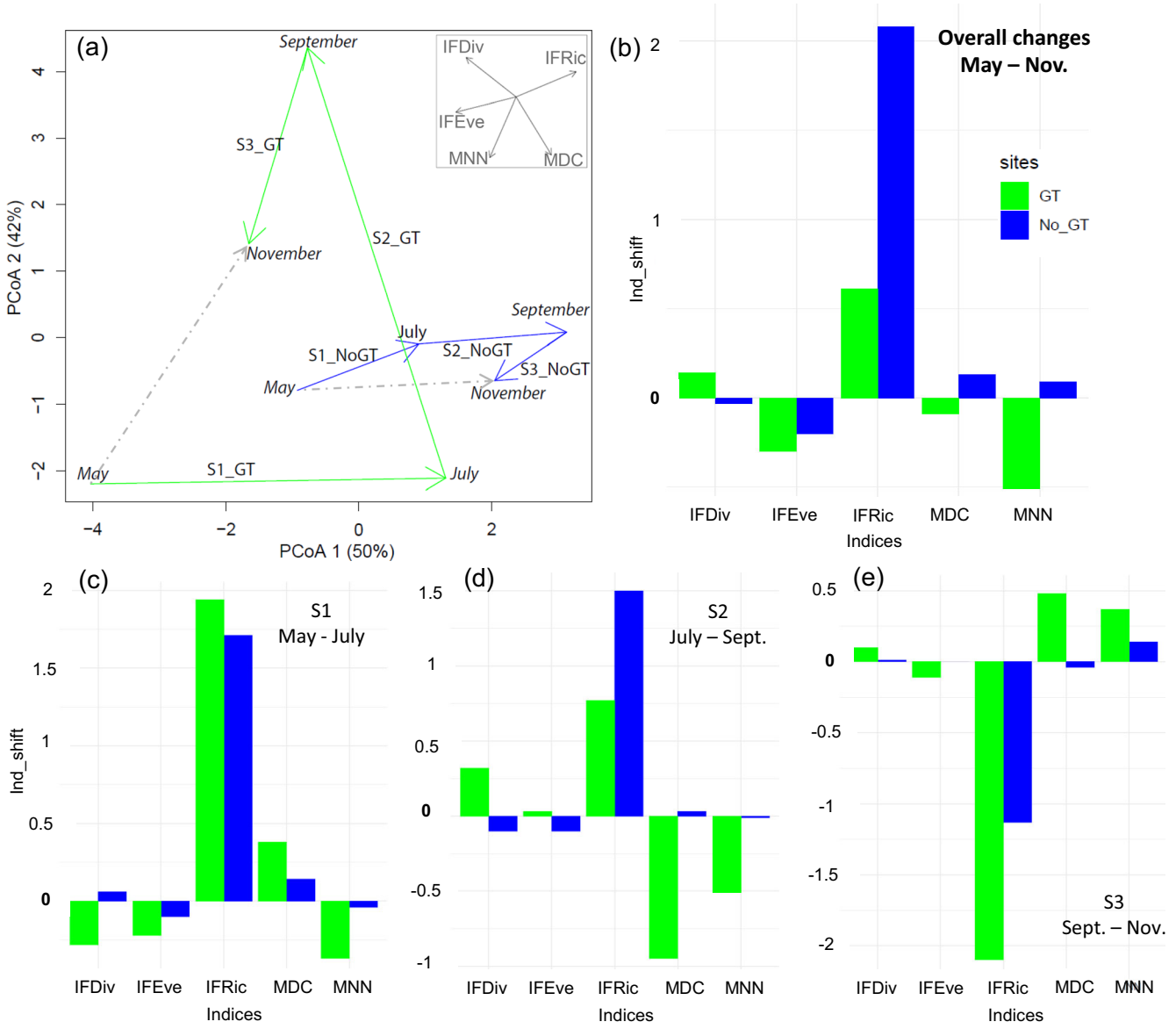

FIGURE 7 Structural and functional trajectories at impacted (green) and pristine (blue) beaches. (a) Trajectory diagram in Ω_γ space. Only two dimensions are shown, representing 92% of the total variance. Solid lines ending with an arrow represent segment lengths and dotted arrow net changes. (b–e) Bar plots represent the shift in value of five structural and functional indices: isotopic functional richness (IFRic), evenness (IFEve), divergence (IDFiv), and mean distance to nearest neighbor (MNN), and centroid (MDC). Bar plot panels show changes in indices values between May and November (b) and for all pairs of consecutives periods (c: May to July, d: July to September, e: September to November). Data from Quillien et al. (2016)

(Bannar-Martin et al., 2018). Environmental changes strongly affect the way species interact and how communities assemble and it is therefore important to assess how the trophic structure of communities will respond to these changes.

Methods

This question was investigated by quantifying the temporal dynamic of the trophic structure of fish communities in a network of gravel pit lakes displaying varying levels of biological invasions (Zhao et al., 2019). Fish were sampled in 2014, 2016, and 2018 using a standardized protocol (gill netting and electrofishing) in six gravel pit lakes located along the Garonne river (Figure 9) (Alp et al., 2016; Evangelista et al., 2017; Zhao et al., 2019). Fish were identified at the species level, counted, measured, and fin clips were collected for $\delta^{13}C$ and $\delta^{15}N$ analyses.

The overall data set (all lakes and sampling year pooled) included 19 species. Five species were present in more than 75% of all communities (18 lakes × years): two non-native species, namely pumpkinseed (*Lepomis*

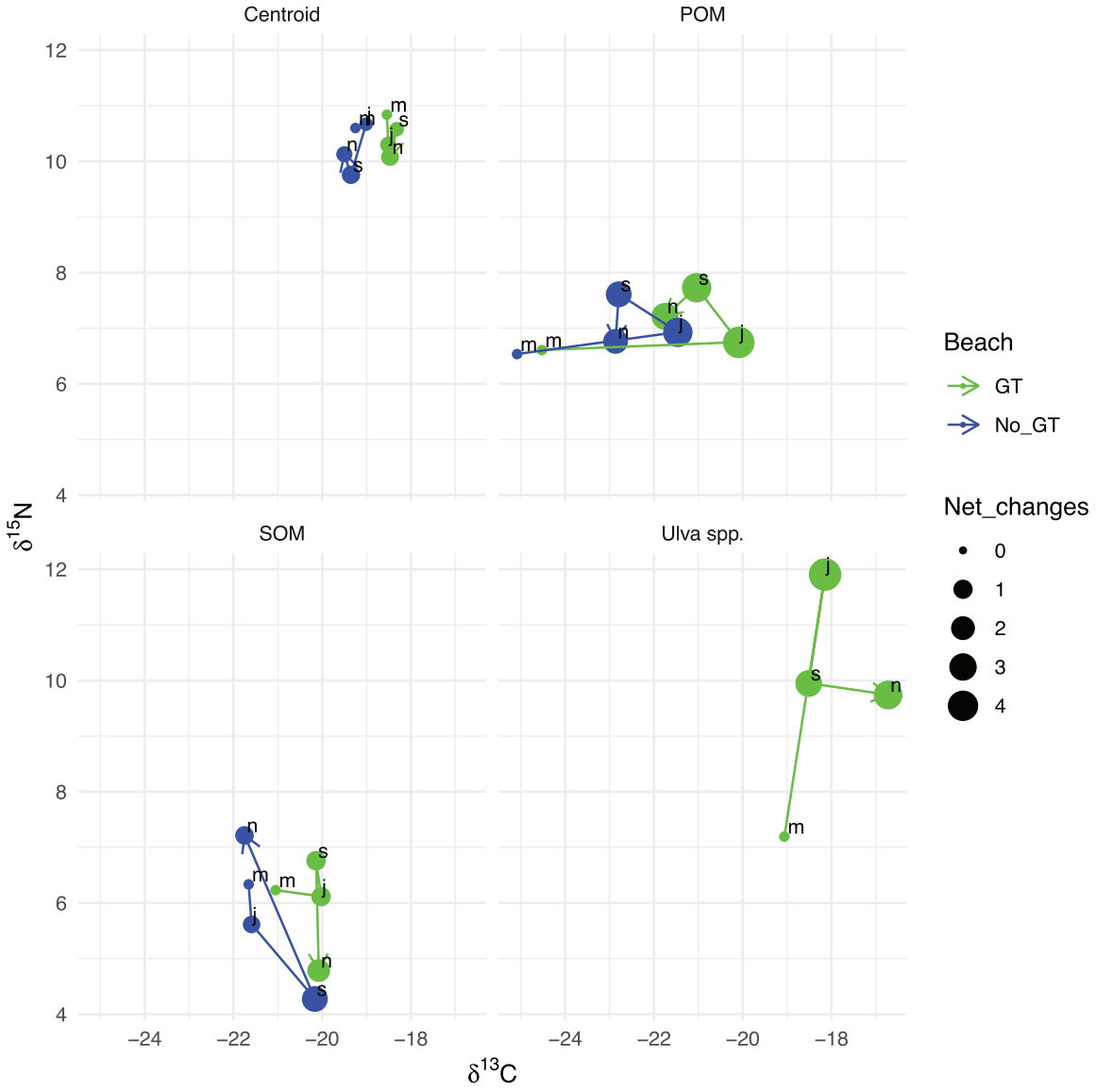

FIGURE 8 Trajectory diagram of food web centroids and basal sources at impacted and pristine beaches. Panels represent specific trajectories for food web centroid, particular organic matter (POM), sedimentary organic matter (SOM), and *Ulva* spp. Size of dots corresponds to net changes, arrows to trajectory path, and colors to beach (GT: green, No_GT: blue). Data from Quillien et al. (2016)

gibbosus) and black bullhead (*Ameiurus melas*) and three native species, namely roach (*Rutilus rutilus*), perch (*Perca fluviatilis*) and rudd (*Scardinius erythrophthalmus*). Rarer species such as *Oncorhynchus mykiss*, *Gymnocephalus cernua*, *Anguilla anguilla*, and others were sampled only for 1 year in one lake. Across all sites and all years, the most abundant species included two invasive species mosquitofish (*Gambusia affinis*) (22.98 ± 18.35%) and black bullhead (17.46 ± 16.37%) followed by the native roach (15.72 ± 14.55%).

The variability of frequency and relative abundance among lakes and years illustrated the strong community dynamics occurring in lakes. A trajectory analysis was performed to determine if changes in community composition were associated to changes in the SI structure of communities over time. Four SI structure indices (namely isotopic richness, $\delta^{13}C$ range, $\delta^{15}N$ range, isotopic evenness following Cucherousset & Villéger, 2015 and Layman et al., 2007) were calculated (Sturbois, Cucherousset, et al., 2021a) using abundance data and used in SITA for Ω_γ. Distance (segment length, net change, trajectory path, NCR, RDT) and direction-based (angle Θ, directionality) were calculated and are represented in TD and maps.

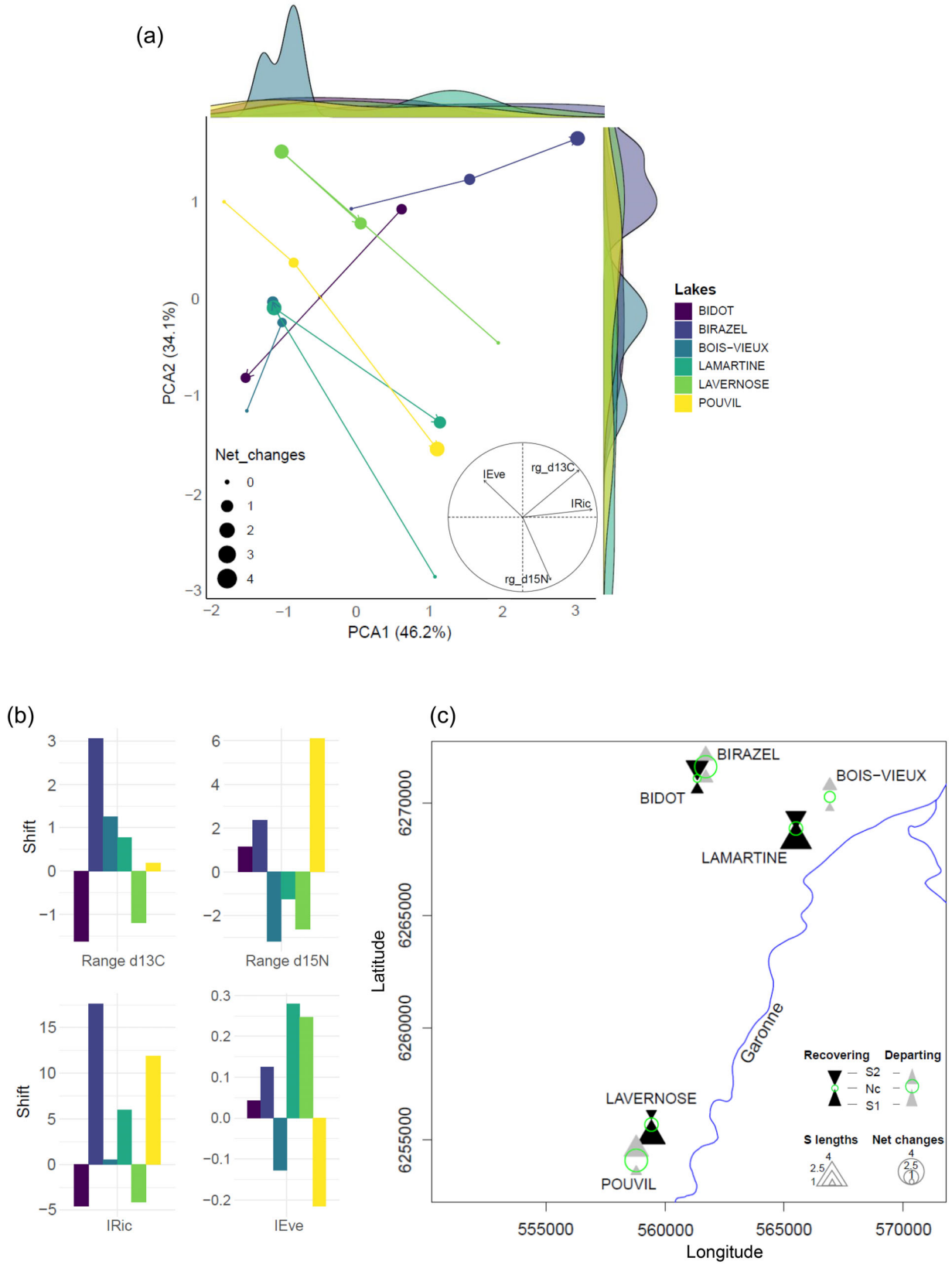

FIGURE 9 Structural trajectories of fish communities in six gravel pit lakes. (a) Trajectory diagram in Ω_γ space. Only two dimensions are displayed, representing 80.3% of the total variance. Bar plots represent the shift in the value of four structural indices: isotopic functional richness (IFRic), evenness (IFEve), and $\delta^{13}C$ and $\delta^{15}N$ ranges. (b) Bar plot panels show changes in indices values. (c) Structural trajectory map: net changes (Nc) are represented with green circles between 2014 and 2018. Bottom triangles represent S1 (2014 to 2016) and top ones S2 (2016 to 2018). The size of the symbols corresponds to segment lengths. For triangles, colors are used to distinguish recovering (black) from departing trajectories (gray)

Results

SITA highlighted a high level of variability between lakes. Lakes Lamartine (trajectory path: 6.70), Lavernose (4.95) and Bidot (4.45) were characterized by a recovering pattern (Figure 9a,c) between 2016 and 2018, as indicated by high angle Θ (146.05°, 164.09°, 172.41°), low DIR (0.19, 0.09, 0.04) and moderate NCR (0.35, 0.48, 0.31) values, respectively. The efficiency of the recovering pattern contributed to low net changes (2.37, 2.37, 1.38). In the opposite, lakes Pouvil (TP: 4.54), Birazel (3.94) and Bois-Vieux (2.90) were characterized by different trajectory patterns characterized by lower angle Θ (63.25°, 16.22°, 100.99°), and higher DIR (0.65, 0.91, 0.44) and NCR (0.88, 0.99, 0.66) values. Differences were also observed in the nature of the structural trajectories among lakes (Figure 9a,b). Specifically, the structural trajectory of Lake Bidot was mainly characterized by a decrease in the $\delta^{13}C$ range, contrasting with Lake Birazel trajectories that were mainly characterized by a strong increase in $\delta^{13}C$ range and isotopic richness, and a moderate increase in $\delta^{15}N$ range and isotopic evenness. We also found that the structural trajectories of Lake Pouvil were primarily characterized by a strong increase in $\delta^{15}N$ range and isotopic richness and a decrease in evenness.

Discussion

SITA approach provided a global and quantitative analysis to compare the magnitude and nature of structural change over time and across multiple lakes with different invasion levels. Coupling distance and direction-based metrics underlined the recovering and departing trajectories characterized by contrasting changes in isotopic indices. In some lakes, exhibiting departing trajectories, direction-based metrics underlined persistent changes through strong linear trajectories, while potential cyclic dynamics were suggested for recovering lakes over the study period. The TM constitutes a synthesis of distance-based metrics and an efficient way to compare the structural food web variability of all lakes. The SITA approach could therefore help to understand the patterns of trophic structure variability in disturbed ecosystems.

Spatio-temporal variability of $\delta^{13}C$ and $\delta^{15}N$ modeled isoscapes in the northeast Pacific

Context

Isoscapes are increasingly used to assess the relative trophic position of higher trophic levels, to provide information on the relative productivity of different regions, and they can also be used to track the migration of animals. Despite isoscapes providing a wide distribution of the variations of SI values, this tool is currently limited for the synthetic analysis of SI dynamics.

Methods

Espinasse et al. (2020) tested the application of isoscapes modeled from satellite data to the description of secondary production in the northeast Pacific. Several key parameters (sea surface temperature, sea level anomaly, and chlorophyll *a*) were used as inputs on a general additive model. The output model fits in a 0.25° × 0.25° spatial grid covering the region spanning from 46 to 62°N and from 195 to 235°E and supporting $\delta^{13}C$ and $\delta^{15}N$ isoscapes from 1998 to 2017 (Espinasse, 2020). We subset modeled $\delta^{13}C$ and $\delta^{15}N$ values of a 1° × 1° spatial grid from the original modeled dataset. Isoscapes modeled for 2013, 2015, and 2017 were selected as they were characterized by high SI dynamics and consequently constituted relevant inputs to test our ITM concept. Modeled SI values for which one of the parameter was missing were excluded. Mapping trajectory metrics requires that stations are synchronously surveyed. Consequently, stations where values were missing for one date within each pair of dates (2013–2015 and 2015–2017) were also excluded. The subset of stations supporting SITA was finally composed of 489 and 488 stations for the periods 2013–2015 and 2015–2017, respectively. Segment lengths (2013–2015 and 2015–2017), and angle α were calculated in the modeled 2D Ω_δ space ($\delta^{13}C$/ $\delta^{15}N$) for all stations and periods and used as input in a modeled ITM. RDT and overall NCR were also calculated to qualify departing or recovering patterns between 2015 and 2017 with respect to the $\delta^{13}C$ and $\delta^{15}N$ values modeled in 2013. Additionally, a long-term SITA was performed from 1998 to 2017, using directions and net changes calculated for all pairs of dates (1998–1999, … , 2016–2017) as input for a TH.

Results

Modeled ITM revealed contrasted dynamics between 2013–2015 and 2015–2017 (Figure 10). While differences in the nature of changes (i.e., direction) were highlighted in the ITM, the overall magnitudes of the dynamics were similar (total segment length = 638.90 between 2013 and 2015 vs. 620.41 between 2015 and 2017). A few areas concentrated an important part of the overall dynamics, especially in the southeast part and, to a lesser extent, in

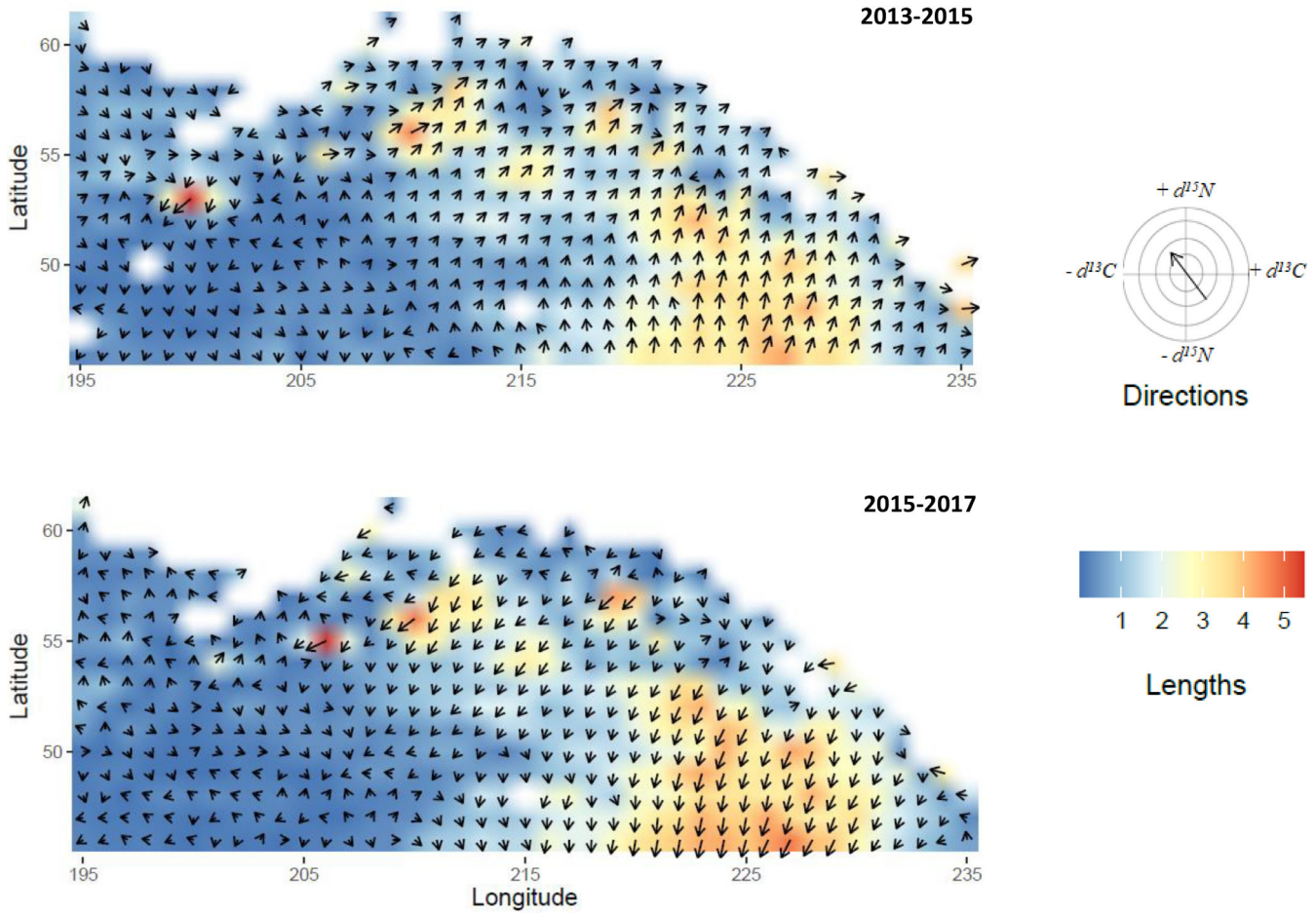

FIGURE 10 Isoscape trajectory maps in the northeast Pacific for the periods 2013–2015 and 2015–2017. SITA metrics were mapped to illustrate stable isotope spatio-temporal dynamics. Direction of arrows (angle α) illustrates direction in the modeled 2D Ω_δ space according to increase and/or decrease in $\delta^{13}C$ and $\delta^{15}N$ values (0–90°: $+\delta^{13}C$ and $+\delta^{15}N$; 90–180°: $+\delta^{13}C$ and $-\delta^{15}N$; 180–270°: $-\delta^{13}C$ and $-\delta^{15}N$; 270–360°: $-\delta^{13}C$ and $+\delta^{15}N$). Length of arrows and colored background rasters illustrate modeled trajectory segment length at each station. Data from Espinasse et al. (2020)

the northern part of the modeled area. The ITMs suggested an overall recovering pattern between 2015 and 2017 with respect to the model defined in 2013, which was confirmed by an RDT < 0 for 76% of stations and a low overall mean of NCR values (0.21).

The TH (Figure 11) revealed that angle α ranging from 0 ° to 90° and 180° to 270° was the most frequent from 1998 to 2017. While SI trajectories characterized by increases in $\delta^{13}C$ and $\delta^{15}N$ values alternated with patterns of decrease in both isotope values and exhibited the major part of the overall changes, some fine scales patterns were also revealed at the beginning of the modeled period.

Discussion

The ITM provides a relevant visual synthesis of (1) spatio-temporal dynamics complementary to (2) modeled isoscapes. (1) ITM, including trajectories of two SI, highlight areas of high variability associated with eddies that enhanced local production in the open ocean (Espinasse et al., 2020). It also allowed the easy identification of areas with SI values that were stable over time, which is useful for animal tracking studies (Trueman & St John Glew, 2019). (2) Modeled isoscapes also illustrate this pattern beyond the decrease in $\delta^{13}C$ and $\delta^{15}N$ values from the coast to offshore (Espinasse et al., 2020). One solution to identify this second pattern in the ITM may exist in the addition of trajectory clusters (color of vectors) from a trajectory similarity analysis. In such cases, users should be careful with the figure readability. The main advantage of this concept of TM lies in its ability to synthesize spatio-temporal dynamics from four isoscapes, which is a major challenge when dealing with massive amounts of spatialized data.

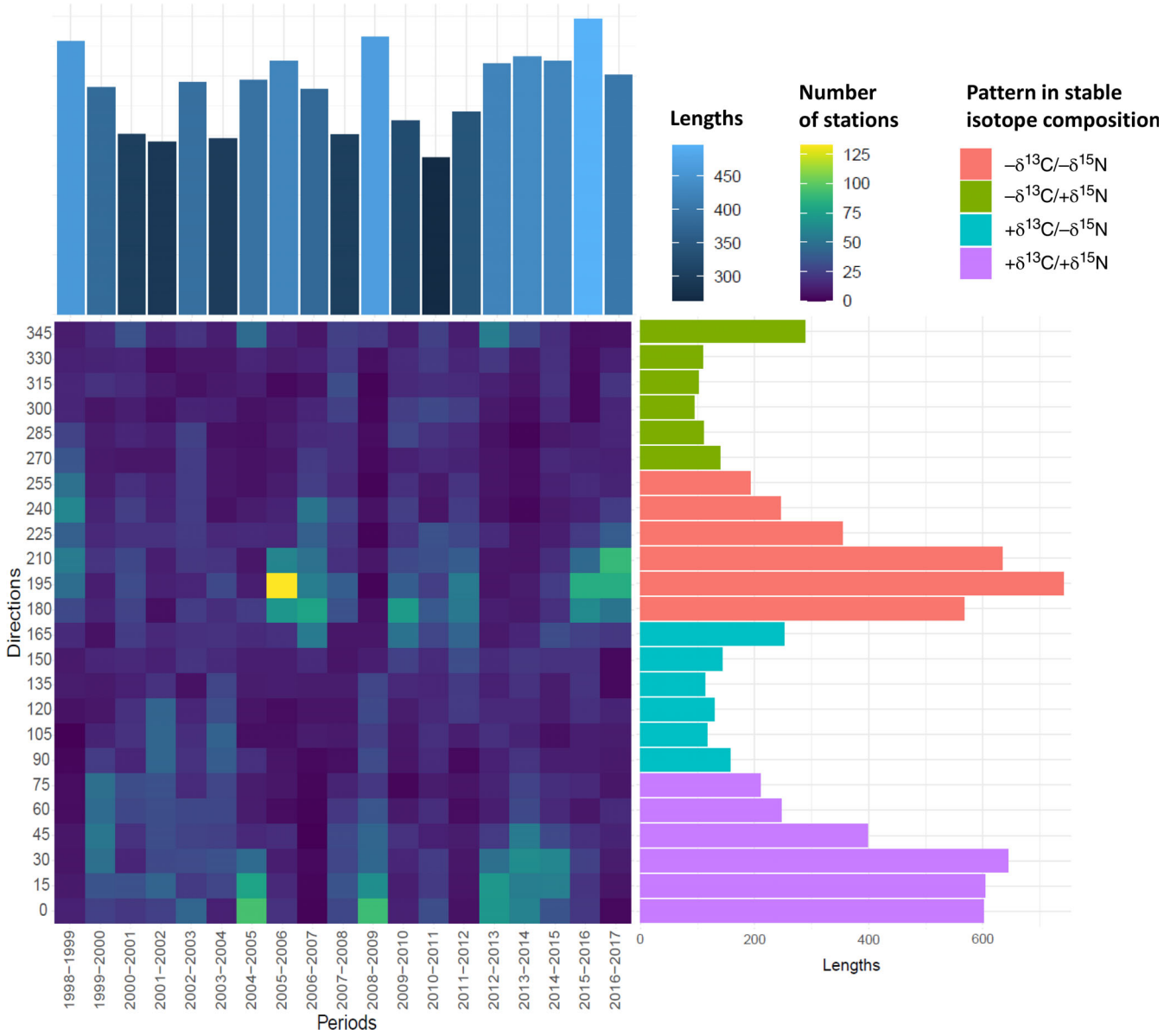

FIGURE 11 Trajectory heatmap. *Heatmap panel*: Angle α in the modeled 2D Ω_δ space exhibited by all stations within all pairs of dates (1998–1999, … , 2016–2017) are represented by the range of direction (15°) according to period. Color gradient from dark blue to yellow indicates the number of stations exhibited by a given range of direction within a given period. *X* barplot: Sum of segment lengths across stations and times, exhibiting the chosen angle. The blue gradient indicates the net change magnitude. *Y* barplot: Overall net changes according to range of directions (angle α). Bars are colored according to increase and/or decrease in $\delta^{13}C$ and $\delta^{15}N$ values (Pink: 0–90°: $+\delta^{13}C$ and $+\delta^{15}N$; Blue: 90–180°: $+\delta^{13}C$ and $-\delta^{15}N$; Red: 180–270°: $-\delta^{13}C$ and $-\delta^{15}N$; Green: 270–360°: $-\delta^{13}C$ and $+\delta^{15}N$). Data from Espinasse et al. (2020)

The TH provides an effective synthesis of high temporal resolution SI dynamics for a 20 years period, highlighting cyclic patterns of enrichment and depletion in ^{13}C and ^{15}N isotopes. Coupled with quantitative SITA metrics, ITM and TH appear as promising tools for isoscapes space–time analyses. These innovative figure concepts allow the illustration of differences in the magnitude and nature of spatio-temporal SI dynamics, and they can be easily coupled with statistics to track accurately significant patterns in high resolutions data sets.

DISCUSSION

Building on previous works dealing with ecological dynamics in SI ecology, we adapted CTA to provide a

formal and explicit framework for the analyses and representations of spatial and temporal trajectories in SI ecology. The different examples used here, sourced from marine, terrestrial, and freshwater ecosystems, illustrate the insights provided by this new analytic framework. SITA originates from the CTA framework, and we believe that the representation solutions proposed here (e.g., trajectory diagrams, TH) are also easily transferable to many different fields of ecology, including community ecology.

Tracking stable isotope dynamics with SITA metrics

Distance- and direction-based metrics provide quantitative synthetic information and allow effective comparisons at the individual, population, community, and ecosystem scales, all being relevant scales that are widely explored in ecology (Layman et al., 2012). Our approach was complementary to original analyses in the different application data sets. Coupled with the calculation of distance- and direction-based metrics, the analysis of trajectory similarity helped to highlight contrasted individual strategies that were not revealed from analysis at the population level, because they did not systematically follow species, age, or gender *a priori* classifications (EA1 and 3). When applied at the individual to the population levels, SITA allows the study of the shape and the magnitude of stable isotope trajectories to track for resource partitioning (EA1), adaptation to a changing environment (EA2, EA3 and EA4), or animal migrations (EA1). The SITA framework allows the measurement of changes in terms of both stable isotope composition (Ω_δ), and structure and functioning (Ω_γ), which is useful and relevant for understanding contrasted food web dynamics in response to environmental or anthropic pressures (EA4). The definition of recovering and departing patterns with respect to initial states highlights different dynamics through the distinction of sites characterized by long-term changes from those characterized by ecological periodicity (EA5), or unexplained, seemingly chaotic, variability. SITA can also identify shifts and cycles in the composition of sources (EA4, EA6). While not illustrated here, using mixing models to define Ω (see p-spaces defined in Newsome et al., 2007) supporting SITA seems a very promising avenue to track temporal changes in the proportion of resources fueling consumers and potential energy pathway dynamics.

SITA contributes to achieving the synthetic challenge inherent to high spatio-temporal resolution datasets, independently of the size of the study area and/or the length of the time series. This ability to deal with large datasets seems especially relevant in the context of isoscape dynamics in widespread and/or intensively studies area, as shown for SI dynamics in the northeast Pacific water body (EA6).

Differences in SITA metrics can be tested statistically as illustrated with circular statistics for direction-based metrics (EA1). Users are encouraged to use complementary statistical approaches, such as regression or correlation tests, to explore the relationship and the strength of the relationship between distance-based metrics and other explanatory variables under natural, anthropogenic, or experimental conditions.

Representing spatio-temporal dynamics in stable isotope ecology

The recent CTA extension (Sturbois et al., 2021) showed the importance of plotting trajectory metrics in specifically designed figure concepts, adapted for the representation of dynamics. Building on this, and on previous attempts in SI ecology (Agostinho et al., 2021; Cucherousset et al., 2013; Schmidt et al., 2007), we proposed here two new figure concepts specifically devoted to the representation of dynamics at large spatio-temporal scales: the ITM and the TH (Figures 10 and 11). Here, we have chosen the figure concepts that we deemed the most suitable for each ecological application. We believe that these entire figure concepts are strongly complementary and that users should explore all figure concepts and metrics, finally selecting the ones most adapted to the relevant hypotheses.

To improve the representation of dynamics through trajectory diagrams, users could innovate in the representation of trajectory metrics. For example, the customization of diagram traditionally used in SI ecology with arrows, density curve, net changes, and trajectory clusters together brings new perspectives in the visualization of ecological dynamics (EA1, EA2, EA4, and EA5). Trajectory roses offer innovative ways to represent directions. We went beyond the arrow diagrams proposed by Schmidt et al. (2007) by using the trajectory rose that allows representation of both angle distribution and length (EA3), or favoring the contrasted distribution of angles among different groups (trajectory cluster, population, anthropogenic factors, etc.) using a circular bar plot structure (EA1). We also developed the initial TM concept (Sturbois et al., 2021) devoted to the representation of trajectory metrics in synthetic maps (EA5), by the proposition of the ITM especially designed to illustrate SI dynamics at very large scales (EA6). Largely inspired by wind and current map, the ITM appears particularly relevant to detect patterns characterized by differences in the nature and magnitude of SI dynamics. To complement the representation of

dynamics at high spatio-temporal resolution, we propose the TH concept, which provides synthetic perspectives to represent both the magnitude and the nature of changes and detect potential long-term SI cycles in large areas (EA6).

We believe that these entire figure concepts are far from being exhaustive and we suggest that users innovate in the representation of trajectory metrics and in the customization of R codes provided here (DataS1: SITA_R_Codes; Sturbois, Cucherousset, et al., 2021b).

Assumption, applications, and limitations of the proposed framework

Ecologists are increasingly using sophisticated methods for dealing with measured data (Fry, 2013) and SI ecology is no exception. While it is always tempting to favor approaches providing quantitative analyses, it is important to keep in mind the biological meaning of associated assumptions, and their inherent simplifications (Layman et al., 2012). If the SITA framework and the associated graphical representations constitute potential management and decision-making tools, we urge users interested in sharing this synthetic tools with stakeholders or managers that interpretation must be done carefully in the hands of experienced multivariate/SI ecologists (Sturbois et al., 2021).

"*A carpenter would never use a screwdriver to pound a nail*" (Layman & Post, 2008): SITA concepts and metrics were not intended as a universal tool to be applied in all situations or as a substitute for other available methods (Buckley, Day, Case, et al., 2021; Buckley, Day, Lear, et al., 2021), but as a new tool for the SI ecologists that could be useful in situations suitable for trajectory analysis. Similar to all analytical tools, there is a high likelihood that the SITA framework may be applied to datasets to which it is not well suited or that inexperienced users may misinterpret the results. Indeed, there is a considerable history of this in the SI literature concerning, for example, mixing models (Fry, 2013; Jackson et al., 2009; Phillips, 2001; Phillips et al., 2014). Users must consequently be aware of the assumptions, fields of application, and limitations associated with the SITA framework as described in this section.

Despite the speed of changes that allows dealing with variations in frequency of surveys, we encourage users to establish sampling strategies, implying synchronous sampling and similar frequency of surveys (De Cáceres et al., 2019; Sturbois, De Cáceres, et al., 2021). It is an essential condition to use at best the SITA framework.

Multivariate ecological methods are descriptive by nature. Despite SITA providing accurate measurements and representations of dynamics in stable isotope ecology, it shares limitations with CTA (De Cáceres et al., 2019; Sturbois et al., 2021). Consequently, SITA outputs must be completed by a strong examination of input datasets (stable isotope raw data or structural and functional indices) to improve the ecological interpretation of observed dynamics. Similarly, SITA may be complemented with additional analyses (Buckley, Day, Case, et al., 2021) to statistically test for other aspects of changes or to provide statistical backgrounds.

Note that ordination spaces are specifically constructed for each given data set. Therefore, any data transformation on the raw data or sampling decision is likely to affect trajectories and, subsequently, all metrics to be calculated. This effect should be tested before any overall transformations of raw data, such as scaling and/or baseline correction of SI values, or any biomass or abundance weighing prior to indices calculation.

Despite the SITA framework being not limited in terms of the number of components considered in metric calculations, some of the applications only considered part of the variability, if Ω_δ or Ω_γ contained more than two dimensions (reporting angles Θ, ω in a 0–360° system, angle α calculation). In this context, performing SITA requires a careful interpretation of the multivariate space to assess the consequences of such reduction.

SITA also shares numerous limitations inherent to stable isotope properties and analysis (Fry, 2008; Garvey & Whiles, 2017). Dynamics of basal source SI values influence the corresponding SI compositions of consumers (Matthews & Mazumder, 2004) and potentially the metrics used to describe the variability, and the food web structure and functioning. However, SITA offers the possibility to explore both source and consumer dynamics. Additionally, many other factors are known to influence food assimilation and finally the isotopic composition of consumers such as fractionation variability or the type of tissue analyzed (Fry, 2008).

In complex ecosystems characterized by similar SI composition of basal sources and in underdetermined cases in which multiple outcomes are feasible from isotope tracer measurements, different feeding pathways may lead to similar positions in δ space (Fry, 2013; Layman et al., 2007), a situation that cannot be disentangled by SITA and necessitates complementary approaches. For the opposite, SITA will be more relevant when differences in stable isotope values of basal sources induce contrasted positions of consumers. When performed at the population level, mean stable isotope values are used as input in SITA, which has the drawback of hiding the stable isotope composition variability at intraspecific levels (Bearhop et al., 2006; Matthews & Mazumder, 2004). In this case, intrapopulation variability could be shown as confidence intervals in trajectory diagrams or maps.

The metrics allow a real-time measurement of dynamics, and a qualitative and quantitative assessment of the potential degree of success in achieving conservations objectives or the impact of natural or anthropogenic changes in environmental conditions. All factors inherent to multivariate and stable isotope analyses, individually or combined, may influence SITA metric calculations, and we urge users for a careful check of such potential bias before defining their sampling design, performing SITA, and interpreting results. Alternatively, conclusions may lead to an incomplete picture and can mislead the description of dynamics with potential misdirecting conservation actions or overstating conservation progress.

Exporting trajectory analysis to other kinds of ecological data

Taking into account the strengths and limitations of the proposed framework, we consider that SITA brings insightful perspectives into the analysis of high-resolution temporal datasets using stable isotopes and/or other tracers in integrating organism tissues. Even though the SITA framework has been here defined based on stable isotope data, and builds on the CTA framework for community data, any other multidimensional input data are likely to be suitable for this approach. For instance, using trajectory analysis on multitrace element data, including SI or not, would provide appealing insights into subpopulation migratory patterns in fish populations based on otolith chemistry (Elsdon et al., 2008; Trueman et al., 2012). Similar applications can easily been foreseen at the individual scale from tree rings, in a dendrochronology context (Sleen et al., 2017), or from environmental signals recorded in bivalves shells (Butler et al., 2019), or bone growth layers (Merrett et al., 2021; Turner Tomaszewicz et al., 2016). As shown at the scale of the northeast Pacific water body (EA 6), sea water SI composition can be tracked to large spatio-temporal scales and may be tested for long-term or seasonal SI trajectories in rain and snowfall (Aizen et al., 2005; Tian et al., 2018), or ice (Schotterer et al., 1997; van Trigt et al., 2002; Werner et al., 2018). Other tracers are also increasingly used in association with SI, such as contaminants (Dietz et al., 2004, 2021) or fatty acids (Madgett et al., 2019), and the absence of limitation in the number of dimensions supporting SITA constitutes an important strength to improve the analysis of such complex multivariate datasets. As experimental studies involve very controlled protocols, SITA metrics can also be particularly relevant to depict experimental trajectories (EA3).

We hope that trajectory analysis using the new *ecotraj* package will contribute to the assessment of natural or man-induced environmental changes using the responses of chemical composition in biological archives, both in contemporary or archeological studies at local, to regional and global, scales. On a broader front, there are claims for an extension of the trajectory analysis concept to other fields in ecology. In this perspective, the adaptability to different type of ecological questions (compositional, functional, structural, trophic, etc.) given by the choice of the space of analysis Ω (i.e., raw variables and dissimilarity metric choice) constitutes the major strength of the approach. We strongly believe that coupling ecological trajectory analysis frameworks with traditional methods of analysis in studies dealing with long-term integrative data sets could bring interesting perspectives for a better understanding of ecosystem functioning, trends in ecosystems quality, and past and present global changes.

ACKNOWLEDGMENTS

We are very grateful to the editor and anonymous reviewers who significantly contributed to improve the quality of the article. We acknowledge the Agence de l'eau Loire-Bretagne (grant number 180212501), the Région Bretagne (grant number OSIRIS PFEA621219CR0530023), the Europe for the European Maritime and Fisheries Fund (grant number FEAMP 621-B) and the Ministère de la transition écologique et solidaire (grant number EJ No. 2102930123) who funded this research as part of the ResTroph Baie de Saint-Brieuc research program. This work was carried out as part of the PhD thesis of A. Sturbois for Université de Bretagne Occidentale. This research was also funded by the Spanish Ministry of Economy (CGL2017-89149-C2-2-R) and all EA were supported by complementary funds described in the respective articles. Particularly, the fur seal work was financially and logistically supported by the French Polar Institute (IPEV, program no. 109, C. Barbraud). The gravel pit lake study was supported by the Office Français de la Biodiversité (STABLELAKE and SOLAKE projects).

CONFLICT OF INTEREST

The authors declare no conflict of interest.

DATA AVAILABILITY STATEMENT

Data are available as follows: Bestion et al. (2019b), Zenodo, https://doi.org/10.5281/ZENODO.3475401; Espinasse et al. (2020), Dryad, https://doi.org/10.5061/DRYAD.D2547D7Z6; Sturbois et al. (2021a), Zenodo, https://doi.org/10.5281/ZENODO.5519696. Code (Sturbois et al., 2021b) is available on Zenodo at https://doi.org/10.5281/ZENODO.5519693.

ORCID

Anthony Sturbois https://orcid.org/0000-0002-9219-4468
Julien Cucherousset https://orcid.org/0000-0003-0533-9479
Miquel De Cáceres https://orcid.org/0000-0001-7132-2080
Nicolas Desroy https://orcid.org/0000-0002-9047-5637
Boris Espinasse https://orcid.org/0000-0002-7490-5588
Yves Cherel https://orcid.org/0000-0001-9469-9489
Gauthier Schaal https://orcid.org/0000-0003-3860-1517

REFERENCES

Adams, D.C., and M.L. Collyer. 2009. "A General Framework for the Analysis of Phenotypic Trajectories in Evolutionary Studies." *Evolution* 63: 1143–54. https://doi.org/10.1111/j.1558-5646.2009.00649.x

Agostinho, K.F.F., L.R. Monteiro, and A.P.M.D. Beneditto. 2021. "Individual Niche Trajectories in Nesting Green Turtles on Rocas Atoll, Brazil: An Isotopic Tool to Assess Diet Shifts over Time." *Biota Neotropica* 21: e20201099. https://doi.org/10.1590/1676-0611-bn-2020-1099

Aizen, V.B., E. Aizen, K. Fujita, S.A. Nikitin, K.J. Kreutz, and L.N. Takeuchi. 2005. "Stable-Isotope Time Series and Precipitation Origin from Firn-Core and Snow Samples, Altai Glaciers, Siberia." *Journal of Glaciology* 51: 637–54. https://doi.org/10.3189/172756505781829034

Alp, M., J. Cucherousset, M. Buoro, and A. Lecerf. 2016. "Phenological Response of a Key Ecosystem Function to Biological Invasion." *Ecology Letters* 19: 519–27. https://doi.org/10.1111/ele.12585

Austin, M.P. 1977. "Use of Ordination and Other Multivariate Descriptive Methods to Study Succession." *Plant Ecology* 35: 165–75. https://doi.org/10.1007/BF02097067

Bannar-Martin, K.H., C.T. Kremer, S.K.M. Ernest, M.A. Leibold, H. Auge, J. Chase, S.A.J. Declerck, et al. 2018. "Integrating Community Assembly and Biodiversity to Better Understand Ecosystem Function: The Community Assembly and the Functioning of Ecosystems (CAFE) Approach." *Ecology Letters* 21: 167–80. https://doi.org/10.1111/ele.12895

Bearhop, S., R. Phillips, R. McGill, Y. Cherel, D. Dawson, and J. Croxall. 2006. "Stable Isotopes Indicate Sex-Specific and Long-Term Individual Foraging Specialisation in Diving Seabirds." *Marine Ecology Progress Series* 311: 157–64. https://doi.org/10.3354/meps311157

Ben-David, M., R.W. Flynn, and D.M. Schell. 1997. "Annual and Seasonal Changes in Diets of Martens: Evidence from Stable Isotope Analysis." *Oecologia* 111: 280–91. https://doi.org/10.1007/s004420050236

Bestion, E., A. Soriano-Redondo, J. Cucherousset, S. Jacob, J. White, L. Zinger, L. Fourtune, L. Di Gesu, A. Teyssier, and J. Cote. 2019a. "Altered Trophic Interactions in Warming Climates: Consequences for Predator Diet Breadth and Fitness." *Proceedings of the Royal Society B* 286: 20192227. https://doi.org/10.1098/rspb.2019.2227

Bestion, E., A. Soriano-Redondo, J. Cucherousset, S. Jacob, J. White, L. Zinger, and L. Fourtune. 2019b. Raw data for: "Altered Trophic Interactions in Warming Climates: Consequences for Predator Diet Breadth and Fitness", Bestion et al 2019 *Proceedings B*. (Version 1). Zenodo. https://doi.org/10.5281/zenodo.3475402

Black, C.R., and J.W. Armbruster. 2021. "New Method of Isotopic Analysis: Baseline-Standardized Isotope Vector Analysis Shows Trophic Partitioning in Loricariids." *Ecosphere* 12. https://doi.org/10.1002/ecs2.3503

Bolnick, D.I., R. Svanbäck, J.A. Fordyce, L.H. Yang, J.M. Davis, C.D. Hulsey, and M.L. Forister. 2003. "The Ecology of Individuals: Incidence and Implications of Individual Specialization." *The American Naturalist* 161: 1–28. https://doi.org/10.1086/343878

Bouillon, S., R.M. Connolly, and D.P. Gillikin. 2011. "Use of Stable Isotopes to Understand Food Webs and Ecosystem Functioning in Estuaries." In *Treatise on Estuarine and Coastal Science*. 143–73. Elsevier. https://doi.org/10.1016/B978-0-12-374711-2.00711-7

Bowen, G.J. 2010. "Isoscapes: Spatial Pattern in Isotopic Biogeochemistry." *Annual Review of Earth and Planetary Sciences* 38: 161–87. https://doi.org/10.1146/annurev-earth-040809-152429

Buckley, H.L., N.J. Day, B.S. Case, and G. Lear. 2021a. "Measuring Change in Biological Communities: Multivariate Analysis Approaches for Temporal Datasets with Low Sample Size." *PeerJ* 9: e11096. https://doi.org/10.7717/peerj.11096

Buckley, H.L., N.J. Day, G. Lear, and B.S. Case. 2021b. "Changes in the Analysis of Temporalcommunity Dynamics Data: A 29-Yearliterature Review." *PeerJ* 9: e11250. https://doi.org/10.7717/peerj.11250

Butler, P.G., P.S. Freitas, M. Burchell, and L. Chauvaud. 2019. "Archaeology and Sclerochronology of Marine Bivalves." In *Goods and Services of Marine Bivalves*, edited by A.C. Smaal, J. G. Ferreira, J. Grant, J.K. Petersen, and Ø. Strand, 413–44. Cham: Springer International Publishing. https://doi.org/10.1007/978-3-319-96776-9_21

Cherel, Y., L. Kernaléguen, P. Richard, and C. Guinet. 2009. "Whisker Isotopic Signature Depicts Migration Patterns and Multi-Year Intra- and Inter-Individual Foraging Strategies in Fur Seals." *Biology Letters* 5: 830–2. https://doi.org/10.1098/rsbl.2009.0552

Connolly, R.M., M.A. Guest, A.J. Melville, and J.M. Oakes. 2004. "Sulfur Stable Isotopes Separate Producers in Marine Food-Web Analysis." *Oecologia* 138: 161–7. https://doi.org/10.1007/s00442-003-1415-0

Cucherousset, J., and S. Villéger. 2015. "Quantifying the Multiple Facets of Isotopic Diversity: New Metrics for Stable Isotope Ecology." *Ecological Indicators* 56: 152–60. https://doi.org/10.1016/j.ecolind.2015.03.032

Cucherousset, J., J.-M. Paillisson, and J.-M. Roussel. 2013. "Natal Departure Timing from Spatially Varying Environments Is Dependent of Individual Ontogenetic Status." *Naturwissenschaften* 100: 761–8. https://doi.org/10.1007/s00114-013-1073-y

De Cáceres, M., 2019. "Package'vegclust'. cran.r-package."

De Cáceres, M., L. Coll, P. Legendre, R.B. Allen, S.K. Wiser, M. Fortin, R. Condit, and S. Hubbell. 2019. "Trajectory Analysis in Community Ecology." *Ecological Monographs* 89: e01350. https://doi.org/10.1002/ecm.1350

Dietz, R., F. Riget, K. Hobson, M. Heidejorgensen, P. Moller, M. Cleemann, J. Deboer, and M. Glasius. 2004. "Regional and Inter Annual Patterns of Heavy Metals, Organochlorines and Stable Isotopes in Narwhals (Monodon Monoceros) from West Greenland." *Science of the Total Environment* 331: 83–105. https://doi.org/10.1016/j.scitotenv.2004.03.041

Dietz, R., J.-P. Desforges, F.F. Rigét, A. Aubail, E. Garde, P. Ambus, R. Drimmie, M.P. Heide-Jørgensen, and C. Sonne. 2021. "Analysis of Narwhal Tusks Reveals Lifelong Feeding Ecology and Mercury Exposure." *Current Biology* 31: 2012–2019.e2. https://doi.org/10.1016/j.cub.2021.02.018

Doucett, R.R., J.C. Marks, D.W. Blinn, M. Caron, and B.A. Hungate. 2007. "Measuring Terrestrial Subsidies to Aquatic Food Webs Using Stable Isotopes of Hydrogen." *Ecology* 88: 1587–92. https://doi.org/10.1890/06-1184

Elsdon, T., B. Wells, S. Campana, B. Gillanders, C. Jones, K. Limburg, D. Secor, S. Thorrold, and B. Walther. 2008. "Otolith Chemistry to Describe Movements and Life-History Parameters of Fishes: Hypotheses, Assumptions, Limitations and Inferences." In *Oceanography and Marine Biology, Oceanography and Marine Biology - An Annual Review*, edited by R. Gibson, R. Atkinson, and J. Gordon, 297–330. CRC Press. https://doi.org/10.1201/9781420065756.ch7

Espinasse, B. 2020. "Data from: Defining Isoscapes in the Northeast Pacific as an Index of Ocean Productivity." Dryad, Dataset. https://doi.org/10.5061/dryad.d2547d7z6

Espinasse, B., B.P.V. Hunt, S.D. Batten, and E.A. Pakhomov. 2020. "Defining Isoscapes in the Northeast Pacific as an Index of Ocean Productivity." *Global Ecology and Biogeography* 29: 246–61. https://doi.org/10.1111/geb.13022

Evangelista, C., A. Lecerf, J.R. Britton, and J. Cucherousset. 2017. "Resource Composition Mediates the Effects of Intraspecific Variability in Nutrient Recycling on Ecosystem Processes." *Oikos* 126: 1439–50. https://doi.org/10.1111/oik.03787

Fry, B. 2008. *Stable Isotope Ecology*, Corrected as of 3rd printing editon, Environmental Science. New York: Springer.

Fry, B. 2013. "Minmax Solutions for Underdetermined Isotope Mixing Problems: Reply to Semmens et al. (2013)." *Marine Ecology Progress Series* 490: 291–4. https://doi.org/10.3354/meps10536

Garvey, J.E., and M. R. Whiles 2017. *Trophic Ecology*.

Guzzo, M.M., G.D. Haffner, S. Sorge, S.A. Rush, and A.T. Fisk. 2011. "Spatial and Temporal Variabilities of δ13C and δ15N within Lower Trophic Levels of a Large Lake: Implications for Estimating Trophic Relationships of Consumers." *Hydrobiologia* 675: 41–53. https://doi.org/10.1007/s10750-011-0794-1

Hudson, A., and H. Bouwman. 2007. "Different Land-Use Types Affect Bird Communities in the Kalahari, South Africa." *African Journal of Ecology* 45: 423–30. https://doi.org/10.1111/j.1365-2028.2006.00750.x

Jackson, A.L., R. Inger, S. Bearhop, and A. Parnell. 2009. "Erroneous Behaviour of MixSIR, a Recently Published Bayesian Isotope Mixing Model: A Discussion of Moore & Semmens (2008)." *Ecology Letters* 12: E1–5. https://doi.org/10.1111/j.1461-0248.2008.01233.x

Kernaléguen, L., B. Cazelles, J.P.Y. Arnould, P. Richard, C. Guinet, and Y. Cherel. 2012. "Long-Term Species, Sexual and Individual Variations in Foraging Strategies of Fur Seals Revealed by Stable Isotopes in Whiskers." *PLoS One* 7: e32916. https://doi.org/10.1371/journal.pone.0032916

Kernaléguen, L., J.P.Y. Arnould, C. Guinet, and Y. Cherel. 2015. "Determinants of Individual Foraging Specialization Inlarge Marine Vertebrates, the Antarctic Andsubantarctic Fur Seals." *Journal of Animal Ecology* 84: 1081–91.

Kline, T.C., Jr., J.J. Goering, O.A. Mathisen, P.H. Poe, P.L. Parker, and R.S. Scalan. 1993. "Recycling of Elements Transported Upstream by Runs of Pacific Salmon: II. δ^{15}N and δ^{13}C Evidence in the Kvichak River Watershed, Bristol Bay, Southwestern Alaska." *Canadian Journal of Fisheries and Aquatic Sciences* 50: 2350–65. https://doi.org/10.1139/f93-259

Layman, C.A., and D.M. Post. 2008. "Can Stable Isotope Ratios Provide for Community-Wide Measures of Trophic Structure? Reply." *Ecology* 89: 2358–9. https://doi.org/10.1890/08-0167.1

Layman, C.A., D.A. Arrington, C.G. Montaña, and D.M. Post. 2007. "Can Stable Isotope Ratios Provide for Community-Wide Measures of Trophic Structure?" *Ecology* 88: 42–8. https://doi.org/10.1890/0012-9658(2007)88[42:CSIRPF]2.0.CO;2

Layman, C.A., M.S. Araujo, R. Boucek, C.M. Hammerschlag-Peyer, E. Harrison, Z.R. Jud, P. Matich, et al. 2012. "Applying Stable Isotopes to Examine Food-Web Structure: An Overview of Analytical Tools." *Biological Reviews* 87: 545–62. https://doi.org/10.1111/j.1469-185X.2011.00208.x

Legendre, P., and B. Salvat. 2015. "Thirty-Year Recovery of Mollusc Communities after Nuclear Experimentations on Fangataufa Atoll (Tuamotu, French Polynesia)." *Proceedings of the Royal Society B* 282: 20150750. https://doi.org/10.1098/rspb.2015.0750

Madgett, A.S., K. Yates, L. Webster, C. McKenzie, and C.F. Moffat. 2019. "Understanding Marine Food Web Dynamics Using Fatty Acid Signatures and Stable Isotope Ratios: Improving Contaminant Impacts Assessments across Trophic Levels." *Estuarine, Coastal and Shelf Science* 227: 106327. https://doi.org/10.1016/j.ecss.2019.106327

Matthews, B., and A. Mazumder. 2004. "A Critical Evaluation of Intrapopulation Variation of δ13C and Isotopic Evidence of Individual Specialization." *Oecologia* 140: 361–71. https://doi.org/10.1007/s00442-004-1579-2

Matthews, W.J., E. Marsh-Matthews, R.C. Cashner, and F. Gelwick. 2013. "Disturbance and Trajectory of Change in a Stream Fish Community over Four Decades." *Oecologia* 173: 955–69. https://doi.org/10.1007/s00442-013-2646-3

Merrett, D.C., C. Cheung, C. Meiklejohn, and M.P. Richards. 2021. "Stable Isotope Analysis of Human Bone from Ganj Dareh, Iran, ca. 10,100 calBP." *PLoS One* 16: e0247569. https://doi.org/10.1371/journal.pone.0247569

Newsome, S.D., C. Martinez del Rio, S. Bearhop, and D.L. Phillips. 2007. "A Niche for Isotopic Ecology." *Frontiers in Ecology and the Environment* 5: 429–36. https://doi.org/10.1890/060150.1

Peterson, B.J., and B. Fry. 1987. "Stable Isotopes in Ecosystem Studies." *Annual Review of Ecology and Systematics* 18: 293–320. https://doi.org/10.1146/annurev.es.18.110187.001453

Phillips, D.L. 2001. "Mixing Models in Analyses of Diet Using Multiple Stable Isotopes: A Critique." *Oecologia* 127: 166–70. https://doi.org/10.1007/s004420000571

Phillips, D.L., R. Inger, S. Bearhop, A.L. Jackson, J.W. Moore, A.C. Parnell, B.X. Semmens, and E.J. Ward. 2014. "Best Practices for Use of Stable Isotope Mixing Models in Food-Web Studies." *Canadian Journal of Zoology* 92: 823–35. https://doi.org/10.1139/cjz-2014-0127

Quillien, N., M.C. Nordström, G. Schaal, E. Bonsdorff, and J. Grall. 2016. "Opportunistic Basal Resource Simplifies Food Web Structure and Functioning of a Highly Dynamic Marine Environment." *Journal of Experimental Marine Biology and Ecology* 477: 92–102.

Rigolet, C., E. Thiébaut, A. Brind'Amour, and S.F. Dubois. 2015. "Investigating Isotopic Functional Indices to Reveal Changes in the Structure and Functioning of Benthic Communities."

Functional Ecology 29: 1350–60. https://doi.org/10.1111/1365-2435.12444

Rubenstein, D.R., and K.A. Hobson. 2019. *Tracking Animal Migration with Stable Isotopes*. Elsevier. https://doi.org/10.1016/C2017-0-01125-4

Schmidt, S.N., J.D. Olden, C.T. Solomon, and M.J.V. Zanden. 2007. "Quantitative Approaches to the Analysis of Stable Isotope Food Web Data." *Ecology* 88: 2793–802. https://doi.org/10.1890/07-0121.1

Schotterer, U., K. Fröhlich, H.W. Gäggeler, S. Sandjordj, and W. Stichler. 1997. "Isotope Records from Mongolian and Alpine Ice Cores as Climate Indicators." In *Climatic Change at High Elevation Sites*, edited by H.F. Diaz, M. Beniston, and R.S. Bradley, 287–98. Dordrecht: Springer Netherlands. https://doi.org/10.1007/978-94-015-8905-5_15

Sleen, P., P.A. Zuidema, and T.L. Pons. 2017. "Stable Isotopes in Tropical Tree Rings: Theory, Methods and Applications." *Functional Ecology* 31: 1674–89. https://doi.org/10.1111/1365-2435.12889

Sturbois, A., M. De Cáceres, M. Sánchez-Pinillos, G. Schaal, O. Gauthier, P. Le Mao, A. Ponsero, and N. Desroy. 2021. "Extending Community Trajectory Analysis: New Metrics and Representation." *Ecological Modelling* 440: 109400. https://doi.org/10.1016/j.ecolmodel.2020.109400

Sturbois, A., J. Cucherousset, M. De Cáceres, N. Desroy, P. Riera, A. Carpentier, N. Quillien, et al. 2021a. Raw data for: Stable Isotope Trajectory Analysis (SITA): A New Approach to Quantify and Visualize Dynamics in Stable Isotope Studies. Sturbois et al., in press in Ecological Monographs. [Data set]. Zenodo. https://doi.org/10.5281/ZENODO.5519696

Sturbois, A., J. Cucherousset, M. De Cáceres, N. Desroy, P. Riera, A. Carpentier, N. Quillien, et al. 2021b. R Codes for: Stable Isotope Trajectory Analysis (SITA): A New Approach to Quantify and Visualize Dynamics in Stable Isotope Studies. Sturbois et al., in press in Ecological Monographs. Zenodo. https://doi.org/10.5281/ZENODO.5519693

Tian, C., L. Wang, K.F. Kaseke, and B.W. Bird. 2018. "Stable Isotope Compositions (δ2H, δ18O and δ17O) of Rainfall and Snowfall in the Central United States." *Scientific Reports* 8: 6712. https://doi.org/10.1038/s41598-018-25102-7

van Trigt, R., H.A.J. Meijer, A.E. Sveinbjörnsdóttir, S.J. Johnsen, and E.R.Th Kerstel. 2002. "Measuring Stable Isotopes of Hydrogen and Oxygen in Ice by Means of Laser Spectrometry: The Bølling Transition in the Dye-3 (South Greenland) Ice Core." *Annals of Glaciology* 35: 125–30. https://doi.org/10.3189/172756402781816906

Trueman, C.N., and K. St John Glew. 2019. "Chapter 6 - Isotopic Tracking of Marine Animal Movement." In *Tracking Animal Migration with Stable Isotopes (Second Edition)*, edited by K.A. Hobson and L.I. Wassenaar, 137–72. Academic Press. https://doi.org/10.1016/B978-0-12-814723-8.00006-4

Trueman, C.N., K.M. MacKenzie, and M.R. Palmer. 2012. "Identifying Migrations in Marine Fishes through Stable-Isotope Analysis." *Journal of Fish Biology* 81: 826–47. https://doi.org/10.1111/j.1095-8649.2012.03361.x

Turner Tomaszewicz, C.N., J.A. Seminoff, L. Avens, and C.M. Kurle. 2016. "Methods for Sampling Sequential Annual Bone Growth Layers for Stable Isotope Analysis." *Methods in Ecology and Evolution* 7: 556–64. https://doi.org/10.1111/2041-210X.12522

Turner, T.F., M.L. Collyer, and T.J. Krabbenhoft. 2010. "A General Hypothesis-Testing Framework for Stable Isotope Ratios in Ecological Studies." *Ecology* 91: 2227–33. https://doi.org/10.1890/09-1454.1

Villéger, S., N.W.H. Mason, and D. Mouillot. 2008. "New Multidimensional Functional Diversity Indices for A Multifaceted Framework in Functional Ecology." *Ecology* 89: 2290–301. https://doi.org/10.1890/07-1206.1

Wantzen, K.M., F. de Arruda Machado, M. Voss, H. Boriss, and W. J. Junk. 2002. "Seasonal Isotopic Shifts in Fish of the Pantanal Wetland, Brazil." *Aquatic Sciences* 64: 239–51. https://doi.org/10.1007/PL00013196

Werner, M., J. Jouzel, V. Masson-Delmotte, and G. Lohmann. 2018. "Reconciling Glacial Antarctic Water Stable Isotopes with Ice Sheet Topography and the Isotopic Paleothermometer." *Nature Communications* 9: 3537. https://doi.org/10.1038/s41467-018-05430-y

West, J.B., A. Sobek, and J.R. Ehleringer. 2008. "A Simplified GIS Approach to Modeling Global Leaf Water Isoscapes." *PLoS One* 3: e2447. https://doi.org/10.1371/journal.pone.0002447

Whitledge, G.W., and C.F. Rabeni. 1997. "Energy Sources and Ecological Role of Crayfishes in an Ozark Stream: Insights from Stable Isotopes and Gut Analysis." *Canadian Journal of Fisheries and Aquatic Sciences* 54: 2555–63. https://doi.org/10.1139/f97-173

Zapata-Hernández, G., J. Sellanes, Y. Letourneur, C. Harrod, N.A. Morales, P. Plaza, E. Meerhoff, et al. 2021. "Tracing Trophic Pathways through the Marine Ecosystem of Rapa Nui (Easter Island)." *Aquatic Conservation: Marine and Freshwater Ecosystems* 31: 304–23. https://doi.org/10.1002/aqc.3500

Zhao, T., S. Villéger, and J. Cucherousset. 2019. "Accounting for Intraspecific Diversity when Examining Relationships between Non-native Species and Functional Diversity." *Oecologia* 189: 171–83. https://doi.org/10.1007/s00442-018-4311-3

SUPPORTING INFORMATION

Additional supporting information may be found in the online version of the article at the publisher's website.

How to cite this article: Sturbois, Anthony, Julien Cucherousset, Miquel De Cáceres, Nicolas Desroy, Pascal Riera, Alexandre Carpentier, Nolwenn Quillien, et al. 2022. "Stable Isotope Trajectory Analysis (SITA): A New Approach to Quantify and Visualize Dynamics in Stable Isotope Studies." *Ecological Monographs* e1501. https://doi.org/10.1002/ecm.1501